*biophysica*

MDPI

*Review*

# Cancellous Skeleton, Microskeleton, Ultramicroskeleton: A Geo/Biomorphological Bone Mineral Microbiome of Hierarchical Force Translation and Ancient Golgi-Directed Lineage

**Jean E. Aaron**

Bone Structural Biology Laboratory, Faculty of Biological Sciences, University of Leeds, Leeds LS2 9JT, UK; j.e.aaron@leeds.ac.uk or jean.e.aaron@googlemail.com

**Abstract:** Bone minerals may be more complex than the prevailing opinion suggests. Understanding its biomaterial properties in health and disease may address fundamental geo/biomorphological ambiguities recurrent within its calcified cancellous hierarchy of macro-, micro-, and nano-skeletal networks. (i) There is evidence that the outer mineral macroskeleton of interconnected trabeculae (150 μm diameter) is modulated according to axes of tensile stress by permeating arrays of periosteal Sharpey's fibres (collagen type III/VI, 5–25 μm thick) studded with tenascin organiser protein. (ii) Its substructural mineral microskeleton is a reticulation of bridged and deformable calcium phosphate/carbonate microspheres (about 1 μm diameter). These organically enshrouded (e.g., bone sialoprotein, osteocalcin, osteopontin) objects, configured by the adhesive organiser protein fibronectin and tempered by trace elements (e.g., Si, Mg, Fe, Al), display differential histochemistry (e.g., acid phosphatase, carbonic anhydrase) and anomalous traits (tetracycline binding, gram-positive microbial staining and nucleic acid staining affinity). The calcified microspheres are intracellular fabrications of osteocyte cohorts developed within "switched on" Golgi cisternae prior to aggregation at the extracellular calcification front in chains and looped assemblies. (iii) Within each microsphere, a less dense centre is encircled by a mineral nanoskeleton of beaded filaments (5 nm in diameter) transmutable in electron density, with a trait for lateral fusion into ladder-like struts, stays and senescent fenestrated plates, constituting domains of microparticle slip and crystal fracture. The evidence suggests a bone mineral biosystem of integrated complexity within which a particulate assemblage at the animate: inanimate calcification front resembles a colonial construct of prokaryote-like, Golgi-fabricated objects calcified with phosphate and harbouring a resident biochemistry. A self-contained "Petrified Microbiome" is proposed to be orchestrated according to a biodynamic primordial paradigm.

**Keywords:** microspheres calcified with phosphate, particulate bone mineral, and geo/bio-morphology; evolutionary mechanobiology; periosteal sharpey's fibres; stressed osteocytes; Golgi apparatus fabrication

check for updates

**Citation:** Aaron, J.E. Cancellous Skeleton, Microskeleton, Ultramicroskeleton: A Geo/Biomorphological Bone Mineral Microbiome of Hierarchical Force Translation and Ancient Golgi-Directed Lineage. *Biophysica* **2024**, *4*, 369–410. https://doi.org/10.3390/biophysica4030026

Academic Editor: Leo Massari

Received: 16 April 2024
Accepted: 26 June 2024
Published: 22 August 2024

**Copyright:** © 2024 by the author. Licensee MDPI, Basel, Switzerland. This article is an open access article distributed under the terms and conditions of the Creative Commons Attribution (CC BY) license (https://creativecommons.org/licenses/by/4.0/).

## 1. Introduction

Big fleas have little fleas
Upon their backs to bite 'em,
And little fleas have lesser fleas,
And so, ad infinitum. (Augustus De Morgan)

Skeletal bone has a diverse history as a biomaterial of choice, ranging from early musical instruments (e.g., a 35,000-years-old flute) to durable tools (e.g., perforated batons for ropemaking). It is a witness to ancient battle scars, deformity and pathology, preserving intrinsic traces of osteocyte networks [1] and ancestral records from post-internment fungi. Without its mineral complement, the flexible organic phase can be effortlessly tied in knots, hence a common "rock and rubber" analogy. Conversely, incineration of the organic phase

does not reduce the remaining material to powder but exposes an inorganic phase (65% by weight) of microarchitectural independence.

At the start of skeletal life, autonomous foetal pumps transfer maternal placental calcium against a concentration gradient to mitigate in-utero rickets and developmental retardation [2]. While bone mass is an established measure of structural strength, less accessible factors define functional "quality" independent of its "quantity". Foremost are microarchitectural and macromolecular properties, especially in tensile regions of vulnerability (wrist, hip and spine) where axially diverse forces of compression and extension combine with transaxial forces of bending, twisting and shear to influence the incidence of fragility factors such as matrix microdamage and fatigue.

While much of the histology of bone is well established [3], the possibility is increasing that the fundamental nature of its hallmark mineral composition may have been underestimated. On the one hand, there is evidence supporting a substance defined by pure extracellular physical chemistry; on the other, it is a material modulated by intracellular intervention. Although bone salt is pivotal to both mineral homeostasis and vertebrate biomechanics, no natural substance has a more deceptive reputation than its closest geo-morphological counterpart "apatite", nominally the "deceiver" from the Greek "apatao" due to certain capricious properties. Extrapolating this to bone tissue are three current anomalies.

(i) The wider biological paradox of bone calcification:

Types of calcium phosphate reported in hard tissues include hydroxyapatite, amorphous calcium phosphate, brushite, whitlockite and octacalcium phosphate. In bone, the inorganic component is widely regarded as small epistatic, collagen-dependent crystals of calcium phosphate permeating an extracellular matrix that is periodically remodelled by cells in response to cytokines and hormones. As such, the calcification event is widely considered to be one of crystal chemistry and inorganic physics, with any biological intervention (such as those attributed to mitochondrial granules and matrix vesicles) being of secondary significance.

Interspersed within this predominantly crystallographic context is occasional reference to bone mineral initiation intracellularly [4], i.e., before its extrusion, in the form of discrete non-crystalline structures, such as are also particularly prominent in calcified cartilage [5]. Doubts were added when traditional preparative procedures were found to alter the bone mineral morphology in comparison to more recent "snap" or "slam" freezing technology [6,7], where mineral disturbance seems minimal. Other non-sequiturs included (i) that "crystallites" may be a rarity in normal young bone where an "amorphous" mineral state is prevalent [8]; (ii) that calcified microspheres, approximately 1 μm in diameter, depart from cultured bone cells at the calcification front [9], while similarly (iii) laser confocal imaging of living growth plate, combined with specific probes and NMR, traced the packaging of calcium phosphate and its passage from chondrocyte to matrix. It follows that (iv) although the inorganic component in vertebrates is compacted with matrix collagen (the surface topography of which sometimes imprints on the mineral under mutual compression), the process of calcification with phosphate is not solely dependent upon a collagen presence. Rather, it occurs in extraskeletal tissues and cells that are devoid of collagen (for example, keratin [10]).

Finally, there is compelling evidence (v) from a commonplace, contractile protozoan observed to gain a substantial musculoskeletal advantage in swimming and burrowing activities by strategically calcifying with phosphate [11] in an intracellular process mediated by tensile scaffolds for mineral assembly [12]. Such observations suggest that a broader biological perspective may produce results about living bone in situ that are at odds with established doctrine. Since the geo/biomorphological nature of the vertebrate skeleton combines an unusual assortment of properties, novel insight may be gained by reference to other tissues and cells that calcify with phosphate and may imply that a significantly wider area of developmental biology has been overlooked.

(ii) The preparative paradox of bone mineral microscopy:

In 1846, Quekett [13] used muriatic acid to remove the "earthy matter" and reported that "ossific substance was composed of small globules". This view, supported by the early granularity assigned to the calcification front by Pommer (1885) [14], was soon to be rejected as a diffraction product of the imperfect optical microscopes of the day (see review by Hancox, [15]). The optical evidence was further demoted by the arrival of the high-resolution electron microscope over a century later.

It has been shown repeatedly in the electron microscope that the extracellular matrix of mature bone (after exposure to manual extraction, dehydration, chemical fixation and image-enhancing density-staining) consists primarily of collagen-dependent sheets of epitactic hydroxyapatite crystals as needles and plates of electron-dense uniformity which permeate collagen fibres and interfibrillary spaces to form a continuum. While reports of "calcospherites", bone "nodules", "globules", and "islands of crystallites" have continued into the contemporary literature, often in relation to membrane-bound matrix vesicles, little mechanical significance has been attached, and such features tend to have been marginalised as transitory phenomena of the calcification front and immature foetal bone.

However, an assumed preparative immutability of bone material may be misplaced. By virtue of its fundamental dynamic function, fresh bone salt in situ may not withstand exposure to manipulation without change, beginning as early as the extraction process. Consistent with this was the recognition in vivo of an "amorphous" (sub-crystalline) state as well as a crystalline chemical one. While optically, the topography of the inorganic phase appears slightly altered by treatment, its ultrastructure seems altogether more tenuous. For example, a simple experiment showed that dehydration of intact murine calvarium generates a typical hydroxyapatite diffraction pattern in the dry specimen in contrast to its absence from the fresh, hydrated control material [16]. Moreover, when technological progress minimises preparation (e.g., hard tissue cryomicrotomy), optical and electron microscopic observation is united, both identifying populations of intracellular and extracellular mineralised microspheres of bacterial dimension.

This seems to explain descriptions by the early histologists in a way that adherence to a uniform crystalline precipitate never has. In addition, it encompasses within bone biology the fabrication of a biomaterial in which the fibrous scaffold of the bone tissue trabeculae visible to the naked eye is intrinsically colonised by populations of calcified microspheres which assemble into a force-related substructure of bone salt trabeculae. If this seems unlikely, the apparent non-stoichiometric nature of the calcium phosphate molecule indicated by its varied hydration characteristics in polarised light perhaps justifies tentative comparison to the uncertain status of Schrodinger's boxed cat "dead or alive" and the challenging quantum conundrum that if the material (i.e., bone salt) can be observed, its natural state is indeterminate, while if its state is determinate, then it cannot be observed.

(iii) The paradox of uncertainty at the bone mineral animate/inanimate interface:

The physical response to skeletal stress is generally acute and inanimate, including fluid flow, matrix strain and spontaneous piezoelectric charge generation passive to crystal deformation. A co-existing animate response has been summarised in the hypothetical bone "mechanostat" model of H.M.Frost, Detroit, in which optimal bone mass meets physical demand by initiation and adjustment of positive or negative remodelling imbalance by osteoclasts and osteoblasts. This remains at the histological forefront as a chronic cycle of cell recruitment and spatial logistics; however, it takes months to accomplish. Complementary but more acute in response may be the ubiquitous osteocyte syncytium equipped with primary cilia, gap junctions and extracellular matrix interconnections along cell integrin pathways. This aspect is in accord with the wider "tensegrity" property of Ingber [17], relating an intrinsic cellular capability to respond to external mechanical forces to the provision of a stabilised environment configured by cytoskeletal nanotubular networks.

The mathematical biologist D'Arcy Thompson was preoccupied with the topographic similarity between animate and inanimate material and the stability gained when natural patterns conform to common mathematical formulae. However, in comparison to synthetic preparations of calcium phosphate, the inorganic phase of bone seems to be deficient in its

obedience to the established laws of physical chemistry. In the living tissue, the interposition of biological energy expenditure at the extensive phosphorylated inanimate/animate interface accelerates an otherwise formulaic progression of inorganic physical chemistry to accomplish in minutes a process that ordinarily takes hours (despite the mediation of collagen epitaxy; F.G.E. Pautard, Leeds, personal communication). In view of the proximal opportunity for cellular intervention, the inorganic phase of bone may be less characteristic of passive precipitate nucleation and more in accord with a dynamic construct of inherent cohesion and capricious deflection, i.e., a bone mineral "microbiome".

The following investigations are recounted in more than 120 articles from my Bone Structural Biology Team at Leeds together with close associates, including a procession of undergraduate students over a fifty-year period since MRC inception, benefitting along the way from milestone advances in technology and cell biology and the exceptional contributions of global visiting scientists and the support of a local biomedical engineer.

## 2. PART I. Bone Mineral Microbiome: Morphogenesis of a Petrified Golgi-Fabrication Fit for Purpose

Approximately 1 micron-sized calcified microspheres populate the mineralisation front to colonise a hierarchical geo/bio-morphological assemblage (i.e., "petrified microbiome") as follows.

(1a) Periosteal portal: Sharpey's fibre arrays propagate transaxial forces.

(1b) Cancellous macroskeleton: defines multiaxial boundaries.

(2a) Cancellous microskeleton: characterised by intracellular Golgi body fabrication of calcified microsphere populations by osteocyte cohorts.

(2b) Cancellous microskeleton: characterised by extracellular calcified microsphere domains and bridged assemblies.

(3) Cancellous ultramicroskeleton: characterised by calcified filamentous clusters.

In the beginning are periosteal arrays of the "perforating fibres" of Sharpey et al., 1867 [18]. It is these to which the cancellous macroskeleton (Figure 1, left) is biomechanically receptive, the intermediary particulate microskeleton is differentially responsive, and the ultramicroskeleton is functionally adapted.

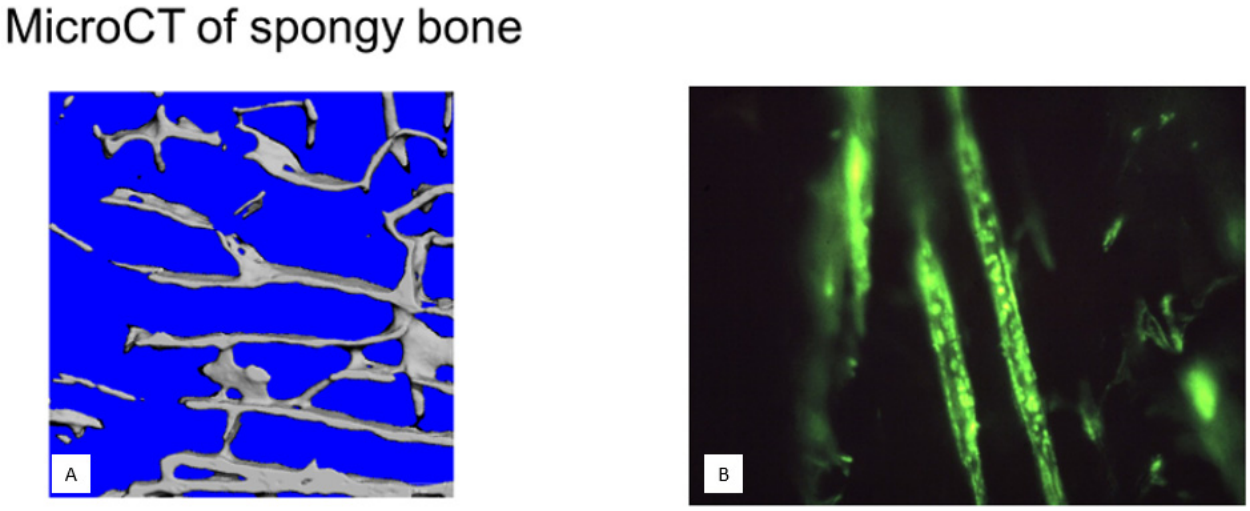


**Figure 1.** (**A**) A typical image of cancellous architecture showing trabeculae approximately 200 microns thick. (**B**) Intraosseous periosteal Sharpey's fibres are approximately 20 microns thick, immunostained for collagen Type III. Preparations by D.H. Carter [19].

### *2.1. Periosteal Portal: Sharpey's Fibre Arrays and Transaxial Force Conduction*

The preliminary support for intramembranous bone begins with the growth from the periosteum (or future endosteum) of arrays of complex birefringent Sharpey's fibres (Figure 1, right) of collagen type III (i.e., CIII), up to 25 microns in diameter, beaded with the

biological organiser glycoprotein tenascin, encircled by elastin and including collagen type VI (i.e., CVI) which notably inhibits their calcification. Traditionally, these perforating fibres provide anchorage for the periosteal membrane (a more pervasive role is recognised in tooth fixation as the Periodontal ligament). Central to their mapping and elevated significance has been the introduction of heavy-duty cryomicrotomes, fresh frozen cryosectioning of undecalcified tissue [19,20], and the advent of specific fluorescent antibody markers. Their distribution seems conducive to extraneous force transduction across a network which traverses the laminated matrix of collagen type I fibres, cement lines and tissue boundaries. A proportion reaches the marrow space to integrate with the narrow (2 μm), uncalcified collagen type III-rich endosteal rim that serves to provide protection from resorption, while others progressively disperse into fine intraosseous filamentous webs.

As embryogenetic products of fibroblast-like cells, Sharpey's fibres form an essential scaffold for osteoblasts and mineral assembly. The resulting primary trabeculae of woven bone align parallel or at right angles to the fibrous arrays depending on location and on the distribution of tenascin (without which dysplasia occurs [19]). Collectively, they present an advancing bone in front of parallel immature bars, which interlink into an open network and fuse into a continuum to complete the first stage of intramembranous development. The second stage expands around intraosseous resorption channels [21] to form typical mature cancellous trabeculae, about 150 μm wide, the Sharpey fibre network persisting as an unmineralised component bonding bone to muscle and mediating exchange at sites of tendon and ligament insertion. In addition, their presence protects the intraosseous regions they occupy from remodelling, thereby crucially conserving insertion stability until old age-related calcification lessens the immunity they provide against negative remodelling imbalance. A positive relationship between Sharpey's fibre number and the corresponding number of muscle insertions has been reported, and like terrestrial muscles, they are apparently disorganised by spaceflight [22–25]. In addition, because they breach anatomical boundaries, their unchecked extension provides a framework for repair (Figure 2). Stimulated by bone fragments (releasing unspecified factors), they bind new bone to old (without the mediation of cartilaginous callus tissue) and forge links with emergent endosteal fibres. This is demonstrated by the exclusively intramembranous trabecular regeneration after an iliac bone biopsy via Sharpey's fibres radially polarised to the cylindrical walls of the extraction space [26].

The occurrence of Sharpey's fibres in tensile strain-resistant intramembranous bone contrasts with their absence from compression-resistant endochondral trabeculae, where septa of collagen type II are colonised directly by groups of prominent mineralised microspheres, each enveloped in the biological organiser protein fibronectin [19]. Some Sharpey's fibres are equipped with unusual accessories, few more remarkable than those impacting the inner boundary (i.e., mid-cortex) of the subperiosteal CIII-rich proximal femoral domain (Figure 3). Here, in orderly alignment (exemplified in a rodent model), are pairs of discrete small, button-like islands of "satellite trapped" cartilage serving as remarkable "flexible hinges" or anchors. Sharpey fibre CVI molecules bond to these vestiges of early development by means of their adhesive groups, enabling internal spatial adjustments at the boundary interface [22]. Another intermediary of intramembranous/endochondral conjunction is a thin physical barrier uniquely shared by CIII and osteopontin in a macromolecular partnership not found elsewhere. The extraneous CIII signal-conduction arriving on one side of this particular frontier is divided from its force-translation on the other in stimulating osteopontin-rich, vascular, remodelling haversian systems. Such extraordinary associations seem to illustrate that the stress-related behaviour of Sharpey's fibres is not to be underestimated.

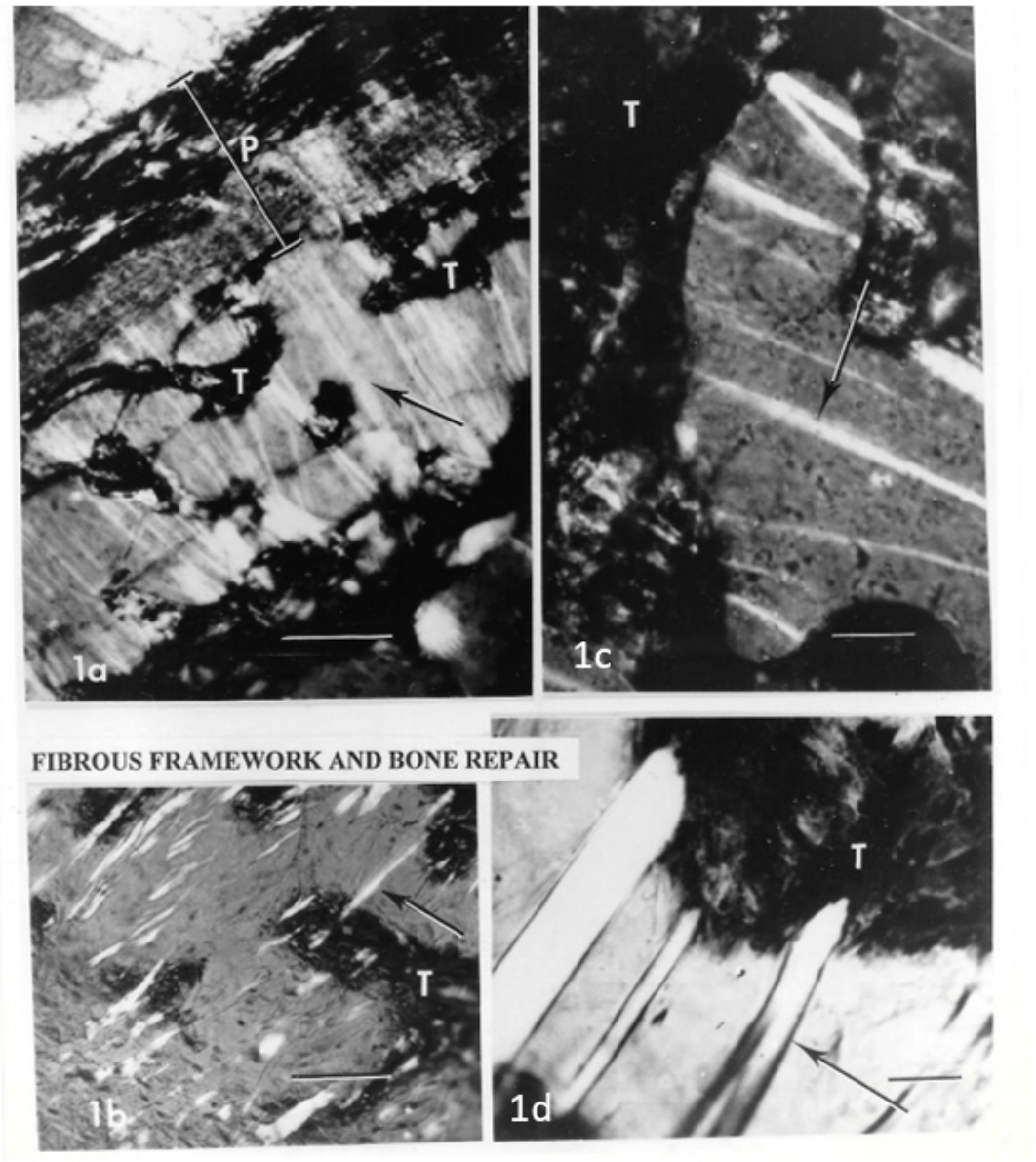


**Figure 2.** Showing the preliminary framework of unmineralised, birefringent periosteal Sharpey's fibre arrays in polarised light, 5–25 μm thick (arrowed), upon which new intramembranous trabecular generation (T) takes place [26]. (**1a**) The developing vertebral body of the foetal lamb where the fibres extend across rudimentary marrow space from the bilaminar periosteum (P). (**1b**) The repairing biopsy site in the sheep ilium 21 days after ablation when the fibres extend across the repopulating marrow space from the endosteum. At both locations, the preliminary framework is central in bonding new bone to old and soft tissues to hard. Von Kossa stain, scale bar (**1a**,**1b**) 100 μm; (**1c**,**1d**) 15 μm.

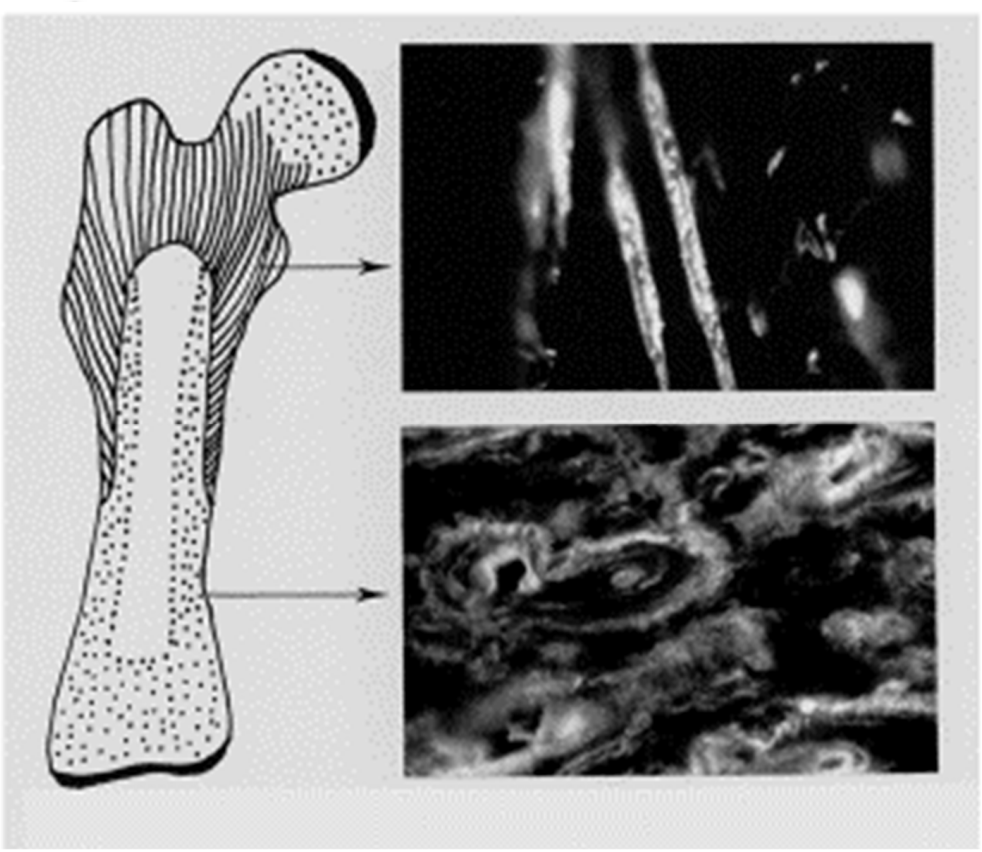

**Figure 3.** In vulnerable locations such as the proximal femur, Sharpey's fibres (immunostained for collagen Type III) are concentrated within a proximal domain (striated). An intervening boundary separates an adjacent domain (stippled) where remodelling is prevalent and rich in osteopontin [27]. Immunostained preparations by D.H. Carter [19] and F. Luther [22]. Archive image. Adapted from Ref [27]. 2003, Advances in Osteoporotic Fracture Management.

### *2.2. Cancellous Macroskeleton (200 µm Gauge): Defines Multiaxial Boundaries*

Cancellous microarchitectural parameters (trabecular volume, width and number) were first measured by simple point- and line-counting procedures, later by computer-assisted automation (e.g., the Quantimet system), and finally expanded to include deductions about trabecular junctions (e.g., Trabecular Analysis System, TAS [28,29]).

Of special morphometric relevance was the trabecular disconnection factor as a measure of cancellous integrity independent of bone mass and a foremost determinant of resilience (Figure 4). To identify, count and map disconnections under the microscope, our simple "in house" (international prize-winning) manual method solved the problem of separating real trabecular termini (ReTm; unstained) from planar histological sectioning artefacts (stained brown) by using thick, plastic-embedded and superficially silver-stained slices (300 µm). These displayed the 2-dimensional cancellous image within its 3-dimensional context, the vertical and horizontal light microscope field coordinates pinpointing their distribution [30]. Application of this method to the evaluation of real trabecular termini (ReTm) in subjects of similar bone mass with and without vertebral fracture demonstrated a mass-independent difference in fragility, with numerous ReTm as a predictor of fracture predisposition more sensitive than any other variable available [31,32].

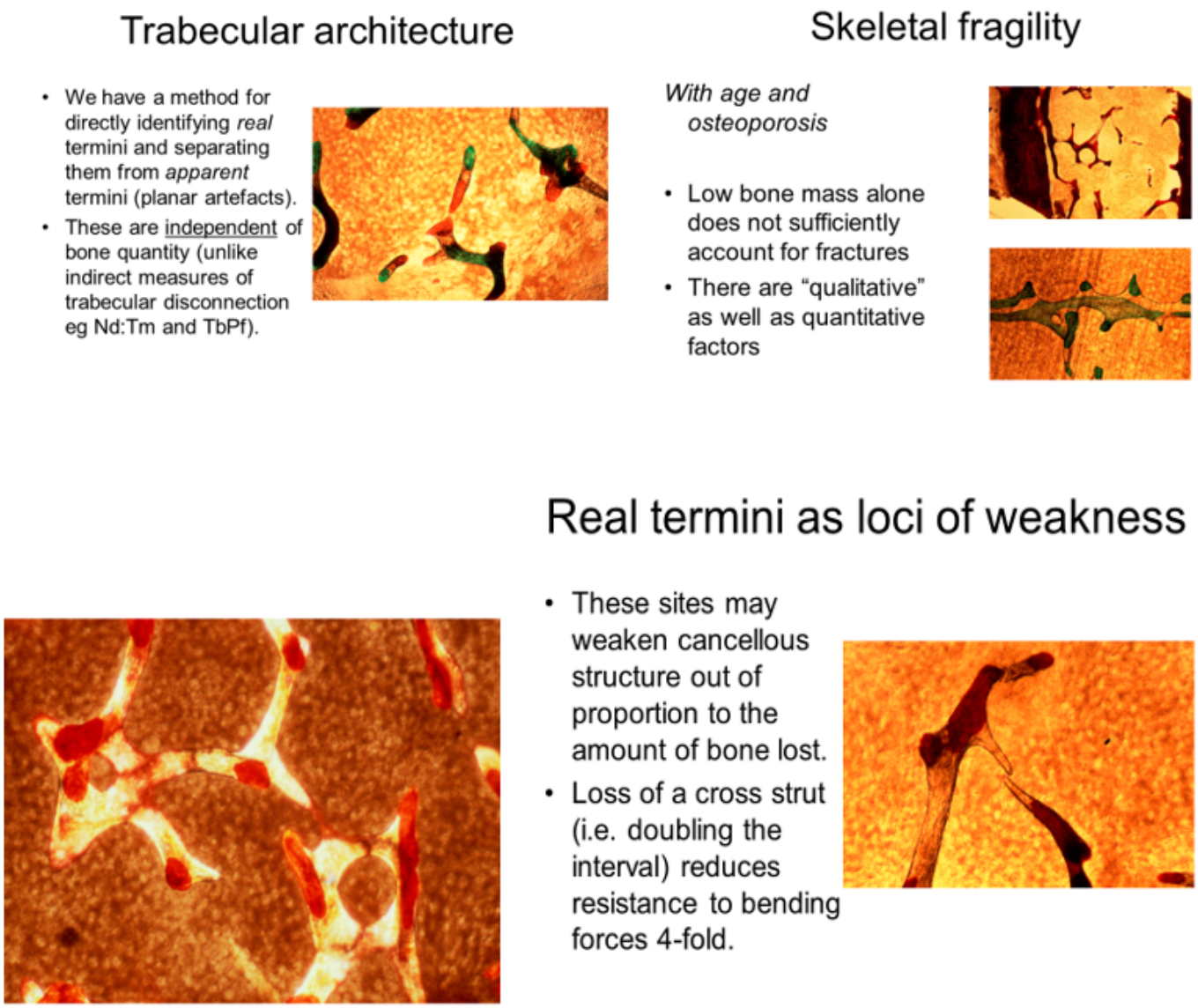


**Figure 4.** Summarising the trabecular disconnection factor as a cause for structural weakness. In cancellous bone slices, the real termini (ReTm, unstained) are separated from planar sectioning artefacts (stained). (**Bottom right**) A transaxial, cross strut, showing the paired, unstained disconnections (i.e., real). Preparations by P.A. Shore [30].

Advances in image-analysis software (Figure 5), in combination with micro-computerised tomography scanning of the plastic-embedded slices, provide 3-dimensional computer-generated constructs of trabecular disconnection, displaying their spatial incidence and collective fracture potential. A transparent 3D cortical shell enclosing the ReTm was generated (Matlab 7.3, Mathworks, Natick, MA, USA) and then refined and validated using the μCT data with overlaid coordinate data [33]. By such means, the evidence suggests that trabecular disconnections become prevalent with age [34], reducing structural strength in excess of the quantity of tissue lost (i.e., doubling the distance between cross-struts causes fourfold weakness). Also, there are 100% more Re Tm in the transverse plane, i.e., on tensile strain-related cross struts, than longitudinally, i.e., on compressed vertical struts.

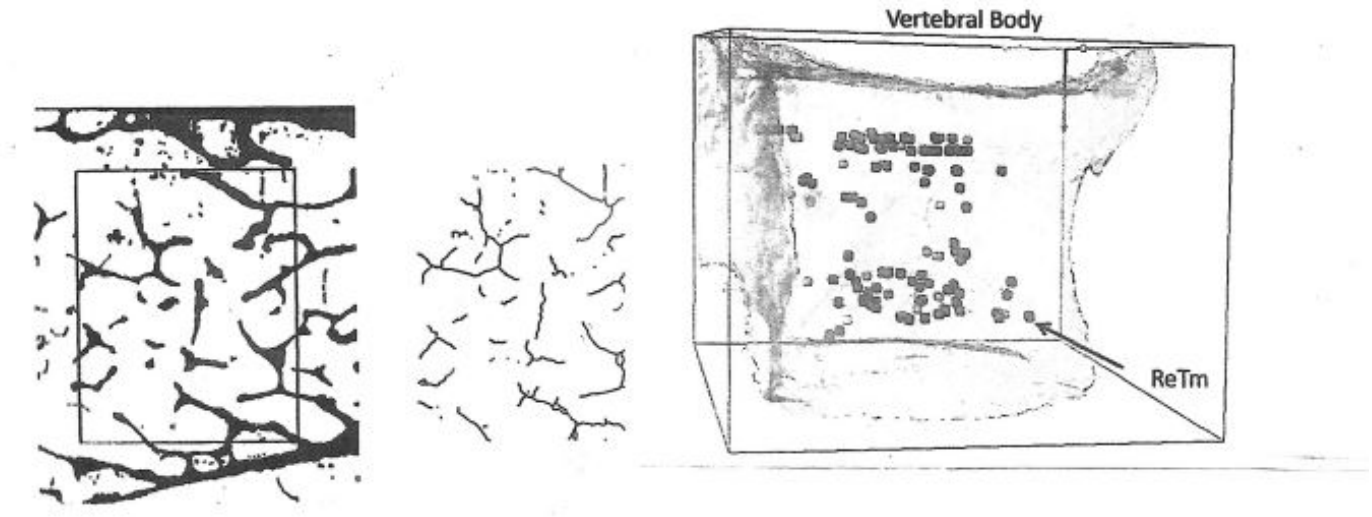


**Figure 5.** Two automated "in house" methods for the analysis of trabecular bone structure. (**Left**) Image shape analysis system driven by a microcomputer (developed by S.K. Paxton and D.R. Johnson [28]). (**Right**) Computer-generated spatial 3D mapping of trabecular disconnection termini (ReTm) in a vertebral body (developed by P. Garner and R. Wilcox [33]). Adapted in part from Ref [28] copyright 1992, Academic Press Inc. and Ref [33], 2013, IBMS BoneKey.

Cancellous network disconnections are rare in youth and tend to be irreversible, except during pregnancy and lactation (see Pregnancy-related disconnection, p.28 for details). Here, their transitory increase is a phase intermediary to a reordered network of thinner, more numerous interconnected bars during late human pregnancy (to which increased serum oestrogen may be proactive). This modulation may better accommodate altered biomechanical pressures during gestation and also metabolic mineral mobilisation during lactation (to which a rise in humoral protective factors calcitonin and vitamin D may be proactive). A gestating animal model has shown a remarkable (40%) increase in cancellous bone volume at the lumbar spine; however, while a single pregnancy strengthens the backbone, a rapid succession of three cycles apparently causes weakness (with the possibility that ex-breeder rats are a convenient model for osteoporosis). The trabecular network dynamics suggest that an increased understanding of the natural mechanisms underlying the positive cancellous outcome of mammalian pregnancy may provide insight into reversing the negative cancellous outcome of menopause.

There is another sex-related difference in the ReTm trabecular disconnection variable. In vertebral bodies and proximal femora of the elderly, ReTm were fewer and more randomly distributed in men than in women. In the latter, they were commonplace and sector-specific, predictably clustering anterior superior (c.f., rare posterior inferior) in vertebrae and distal superior and proximal inferior in the femur [34]. A coincidence is suggested between ReTm distribution and muscle-generated force patterns along axes of the most prominent strain-related trabeculae. Consistent with this is the bone loss and increased ReTm after ovariectomy (using animal models [35]) when previously positive, immunofluorescent Sharpey CIII/VI populated areas apparently become negative [22] prior to the loss of bone. On this basis, ovariectomy relates to the disconnection of trabeculae by truncating the Sharpey's fibres and reducing their sub-periosteal sphere of influence and protection (an effect that may be increased when combined with calcium deficiency [36]). It follows that multi-cross-strut atrophy at disconnection "hotspots" may be the inevitable outcome of a proactive, humoral-induced decline in the morphogenic Sharpey fibre scaffold (Figure 2); this would trigger matrix remodelling and endosteal attrition of previously stabilised locations [12]. The exchange suggests that skeletal Sharpey's fibres may be as essential to the retention of functioning bone within a muscular environment as they are to the retention of functioning teeth within the gums.

### *2.3. Cancellous Microskeleton (1 µm Gauge, Intracellular Event): Characterised by Golgi Body Fabrication of Calcified Microsphere Populations by Osteocyte Cohorts*

Throughout the animal kingdom, calcium phosphate appears as large, enamel-like crystals (usually epidermal and stable), small, elongated crystallites (usually endoskeletal), and non-crystalline, amorphous, subcellular deposits (often loading and unloading in response to mechanical and homeostatic stimuli [16]). "Microsphere" is a geological term chosen by Pautard [37] to encompass the many spherical particles of inorganic calcium salts, 0.1–100 µm diameter, which occur throughout the animal kingdom under a variety of names. Microspheres of calcium phosphate, 0.1 µm in diameter, similar to those found in bone, can be synthesised chemically in an inorganic medium. There, they occur as transitory precipitates from supersaturated synthetic fluids after 40 h under physiological conditions, following which they may transform from an amorphous state to apatite [38–40], and this seems to confirm the basic process in bone. However, the chemistry has to be reconciled with optical observations of bone salt (see review [41]) as an inorganic phase of diverse microsphere populations which persist beyond the calcification front into skeletal maturity and from which they can be isolated by various means for analysis.

Stress-related mineral microsphere fabrication and a protozoan legacy: It is common for the natural history of simple organisms to provide insight into conserved ancient phenomena; in that tradition, it is over half a century since *Spirostomum ambiguum*, a culturally convenient, large, contractile, aquatic protozoan was proposed as a model for the origins of backbones by Pautard [11]. This was due to its predisposition to accumulate and transport bone salt as an initial response to depleting environmental levels of vital phosphate as primordial competition intensified (Figure 6). There followed intracellular, calcified microsphere accumulation, single or bridged, their polarised alignment varying from trans-axial in swimmers to axial in burrowers. During its stressful habit of tunnelling in silt, the cytoplasmic ebb and flow of calcified microspheres converge with contractile muscle "myonemes" to facilitate rudimentary musculoskeletal integration assisted by undefined tensile adhesion (perhaps the hypothetical precursors of the force-translating Sharpey's fibre arrays). The large but fragile cell is effectively protected from destruction by the presence of such microparticles sufficient to withstand exposure to high-pressure chambers [42] and in extremis so packed that axial flexion has been likened to osteoarthritic stiffening. On returning to a less stressful swimming mode, much of its particulate cargo is jettisoned, with a portion recycled as a metabolic mineral reserve. After a period of multiplication, a sedentary phase of mineral depletion may follow, the cells hanging vertically in immobile curtains. Such cytoplasmic mineral conjunction separates *S. ambiguum* from its non-calcifying contemporary *Stentor polymorphus*, which is confined to delicate anchorage and gentle swimming. The transformative dynamics between the pair are resonant of the evolved, active mineral-loading bone cell and its quiescent and unloaded sequel behind the calcification front.

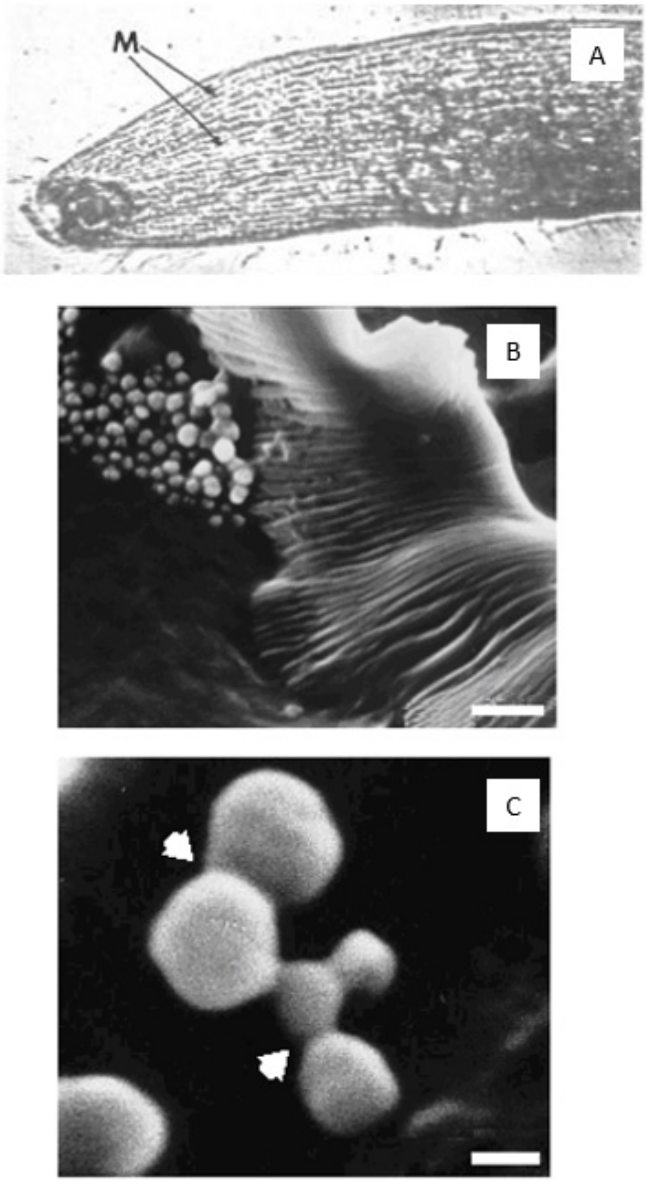


**Figure 6.** The contractile calcifying protozoan *Spirostomum ambiguum* is a model proposed for intracellular bone mineral fabrication by F.G.E. Pautard [43]. The wormlike shape (**A**) is modulated by muscle myonemes (M). When tunnelling in silt (**B**) the organic stack is an interface at which assemble multiple populations of golgi-fabricated microspheres calcified with phosphate, about 1 μm diameter. The calcified objects are released into the cytoplasm (**C**) and align in bridged assemblies (arrowed) relative to stress. Scale bar (**B**) 3 μm; (**C**) 0.5 μm. Preparations by V. Fallon [44]. Archive image.

Stress-related osteocytes: Golgi-directed mineral microsphere fabrication. Subsequent advances in cell biology have enabled the protozoan translator of extraneous forces into mineral particle fabrication to be pinpointed to the juxtanuclear Golgi apparatus, an organelle that is especially elusive in its characterisation. By monitoring the transfection of live organisms in situ with the Green Fluorescent Protein-tagged mannosidase II construct, the specific GFP-tagged Golgi fluorescence marker increased significantly from swimmers to burrowers ($p < 0.0001$). This was synchronous with equally significant juxtanuclear mineral accretion (tetracycline labelled, confirmed by EDX elemental analysis) harvested as dense pellets rich in Ca, P (Ca:P 0.98) and Si. Again, the microparticulate alignment changed from trans-axial in swimmers to axial in burrowers in an apparent demonstration of polarised counteraction pre-empting aspects of the intraosseous event [44].

It follows that when the quiescent bone cell is intermittently energised, the typically compact juxtanuclear body expands to encompass the copious fabrication of micron-sized objects calcified with phosphate (Figure 7). Common to both the adopted protozoan model and the "young" osteocyte is (a) a similar intracellular mineral pattern [45], (b) the same Golgi body association, (c) an unexpected shared expression of identical conserved, cisternal resident proteins (e.g., mannosidase II enzyme or non-mammalian equivalent [46,47]; (d) intermittent biomechanical initiation at the calcification front; (e) a proximal mitochondrial presence facilitating phosphate exchange [48]. Moreover, it seems that all mammalian cells in possession of a Golgi apparatus are likewise equipped with an ancient force-resistant calcification capacity, perhaps evocative of a universal "calcification gene". This finds expression to a greater or lesser degree according to cell type, with evidence in soft as well as hard tissues, and most manifest in the osteocyte lineage [49].

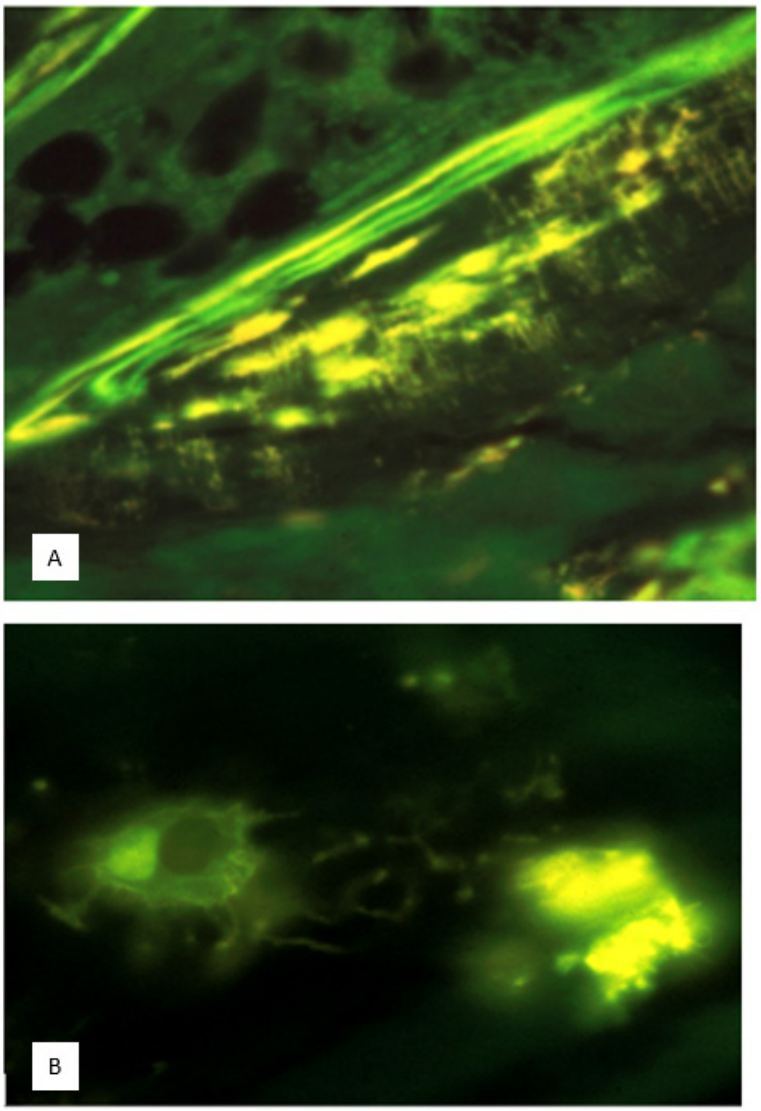


**Figure 7.** (**A**) Osteocyte cohorts at the calcification front stained with tetracycline. (**B**) Osteocytes show a fluorescent "switched on" juxtanuclear Golgi apparatus with cell processes delivering a fluorescent cargo of stained calcified particles (about 1 μm dimension) to the calcification front. UV light [27].

The Golgi apparatus and evolution. First characterised in neurons by Camillo Golgi in 1898 for its unusual argentophilic property, the Golgi apparatus is probably the least understood organelle with its enclosure of unexplored mineral-generating labyrinths. The details exposed by the arrival of the electron microscope and, in particular, its application

to various invertebrate hard materials were of dense calcified objects assembled within its cisternae, providing fresh impetus to the field of mineral biology and elegantly displayed in marine algae. The unicellular coccolithophorids, universally significant as carbon dioxide-fixing organisms, possess distinctive Golgi-membranous, dumbbell-shaped templates which calcify with carbonate [50,51]. Within these customised enclosures, a number of stable, dumbbell-shaped coccoliths, 5 μm in diameter, are formed in 5-min cycles arranged into ectoskeletal shields [51,52]. Other calcified objects have been exemplified in a fresh-water ciliate *Euplotes eurystomus* and in the hepatopancreas of the snail *Helix pomatia* and confirm that their intracellular generation is not extraordinary, neither is it confined to the invertebrates, being a feature of the keratin cells of vertebrate horn and hoof as well as elsewhere in the animal kingdom [10,37,43] and in advanced plants too (e.g., the onion cell Golgi body) such that on this basis the popular *extracellular* view of bone mineral is an exception rather than the rule.

It follows that in the brief, intermittent unloading phase of the Golgi apparatus of the "switched on" osteocyte cohorts, the release of mineral microspheres propels the advancing calcification front at a rate of approximately 1 μm/day (Figure 8). The intracellular histochemical distribution of calcium phosphate (or carbonate using von Kossa, GBHA or tetracycline stain) at optical and ultrastructural levels [53–59] has been observed during normal bone development by several authors [4,60,61]. Validation of such histochemical stains (including tetracycline, which produces a fluorescent complex with bone salt) has been made by EDX (energy dispersive X-ray microanalysis) together with confirmation by others that such calcified objects (for example, Jayasinghe et al. [62]) are biological structures and not artefacts (Rungby et al. [63]). The "nascent" state of early bone salt within precursor "nests" of nanospheres (40–250 nm) indicates the risk of elution without preventative precautions [41,64]. Similar fugitive behaviour has been effectively demonstrated by Wooding and Morgan [65] in studies of the Golgi-directed packaging of calcium for milk production by the lactating mammary gland.

To confirm a hereditary link between bone cells and their postulated protozoan model, the same methods of light and laser confocal microscopy together with electron microscopy and elemental EDX have been repeated by Fallon et al. [44,46] in a comparison of young osteocytes in situ in fresh and "slam" frozen developing mouse calvarium with similar cells (MC3T3-E1; newborn mouse calvarial cells with dendritic processes) maintained in vitro. As in *S. ambiguum*, the location of the "nascent" mineral in the juxtanuclear body was coincident with transfected Golgi apparatus fluorescence with GFP/mannosidase II construct. In substantiation, each Golgi-directed cycle of calcium phosphate/carbonate loading and unloading is about 15 min in duration and not only is it halted by the Golgi body inhibitor brefeldin A, but it is also restarted by the Golgi body stimulant forskolin.

The similarity in intracellular bone salt manipulation between organisms at opposite ends of the evolutionary spectrum suggests that future mechanical implications of this novel biological aspect need to be addressed in terms of the remarkable performance of the Golgi apparatus and the possibility that the microsphere is a universal biological container for calcium phosphate incorporation both within and outside cells. A morphometric approach combines osteocyte network cytoplasmic volume, density and interconnection variables as an indirect measure of Golgi body potential (for example, by tetracycline staining). On this premise, a "switched on" Golgi apparatus, by its nature, occupies an expansive interconnected cytoplasmic cell body, while that of its "switched off" counterpart is correspondingly retracted. Analysis of the 3D osteocyte network (slices 300 μm thick; en bloc stained calcein fluorochrome intracellular marker) captured by an "in house" system devised by Garner and Wilcox combines confocal laser microscopy with image analysis software (ScanIP, Simpleware, Exeter, UK) and novel customised binary masks. These specifically represent cell components by corresponding in-house code (Matlab, Mathworks, Natick, MA, USA), selectively quantitating cell number, length and interconnection [66–68], enabling the objective mapping of osteocyte network translocation and its diversity in health and disease (Figure 9).

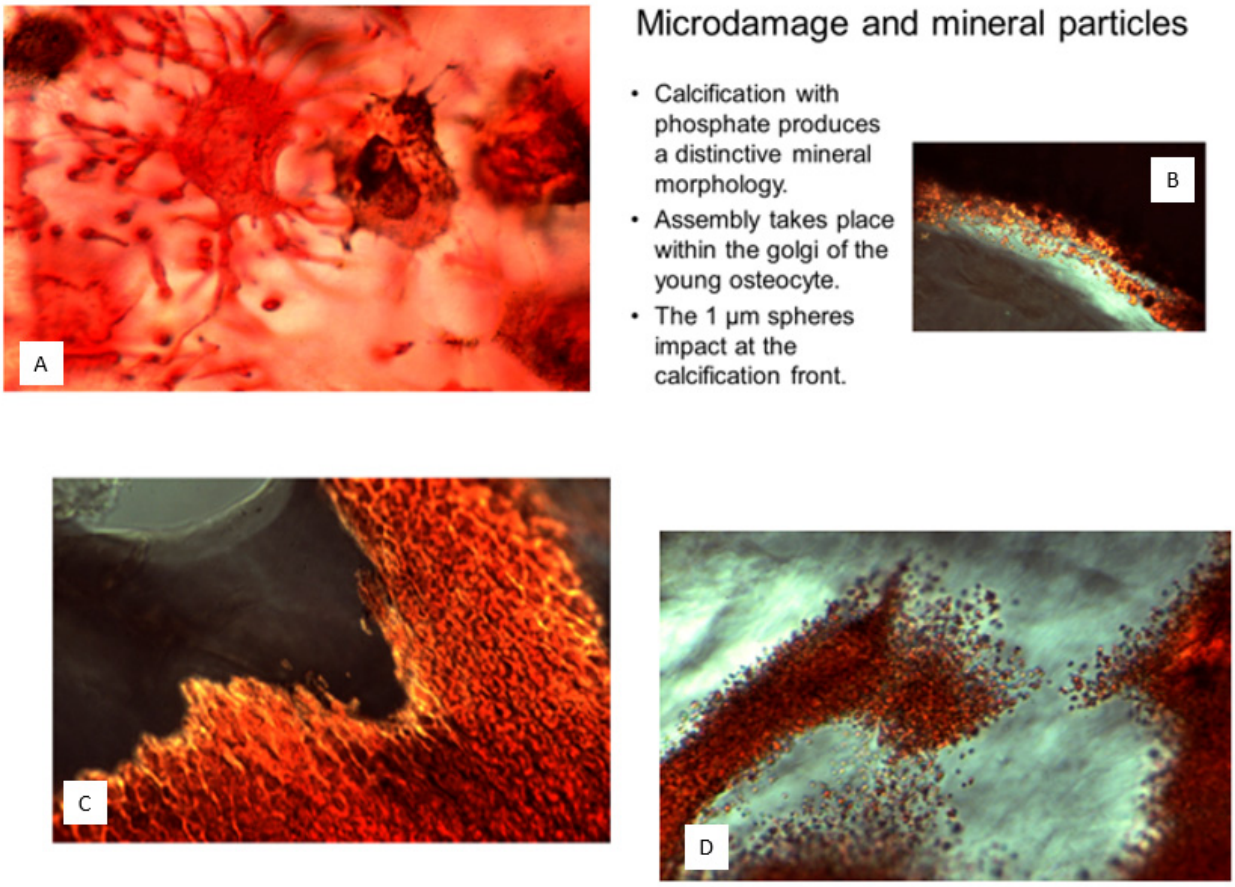


**Figure 8.** (**A**) osteocytes loaded with stained bone mineral microspheres delivered (**B**) to the extracellular calcification front forming bridged assemblies which (**D**) colonise the collagenous matrix in the form of a reticulated microskeleton (**C**). Von Kossa and GBHA stains, Nomarski optics [58]. Adapted from Ref [58]. 1980, Metabolic Bone Disease and Related Research.

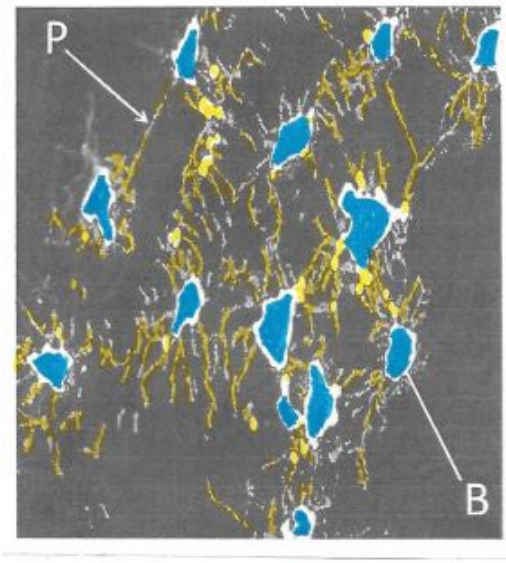


**Figure 9.** Computer-assisted "in house" method for 3D mapping of osteocyte populations to compare regional variability in relation to stress translocation, combining thick slice (300 µm) histology, confocal microscopy and image analysis software (ScanIP, Simpleware, UK) that generates 3d binary masks differentiating cell body (B) and cell process (P) compartments. Preparation by R. Wilcox and P.E. Garner [66]. Reprinted from Ref [66]. 2013, IBMS BoneKey.

### *2.4. Cancellous Microskeleton, Extracellular Event: Characterised by Calcified Microsphere Domains and Bridged Assemblies*

Through some motile mechanism, the intracellular microspheres are positioned at the extracellular calcification front in assemblies and domains before becoming compacted, dehydrated, and distorted. The various examples of intracellular calcification described above combine with bone to illustrate major differences between synthetic and Golgi-directed calcification [37], including the comparative advantage of speed. In particular, there is a large discrepancy between the investiture with mineral in 15 min [56] of an organic intracellular profile, 1 μm in diameter, in one and the need for supersaturation and slow crystal growth over several days in the other. In addressing the role of collagen: firstly, the inorganic independence from collagen is repeated throughout the invertebrate kingdom and, secondly, is supported by the absence of immunostaining for collagen type I in unstained microsphere silhouettes against a fluorescent background in sections [69] and as intact microspheres isolated from bone [70]. Thirdly, scanning electron micrographs show calcium phosphate microspheres, 1 μm in diameter, detaching in quantity from cultured rat bone cells in the absence of collagen and specifically described as "afibrillar" in composition [9]. At the same time, an apparent spatial independence between the collagen fibres and calcified microspheres does not exclude the mutual gain in structural stability of a variable secondary cohesion.

Following extrusion from the osteocyte syncytium, the Golgi-fabricated microspheres populate the extracellular matrix as complex objects of bacterial dimension. The associated and mechanically sensitive mitogenic adhesive protein fibronectin [71] may assist in the interconnection of a proportion of the discrete microspheres and their linkage into chains and looped assemblies (see below) to create a reticulated microskeletal network encircling and aligned to the collagenous matrix bundles (Figure 10). The "micro-trabeculae" (1 μm thick) of the microskeleton are clear under the optical microscope, where polarised light combined with the von Kossa stain enhances their topography not only at the calcification front but also in the mature tissue beyond. In thin optical sections (3 μm thick) of adult bone (stained or unstained under Nomarski optics) and in young, fresh whole tissue mounts (neonatal mouse calvarium), there is evident a maturation sequence from isolated microspheres to bridged assemblies varying regionally in composition, mobility, solubility and differential crystallinity (Figure 11).

Structural and ultrastructural evidence is accumulating consistent with the extracellular matrix as a collagenous framework invested by colonies of microspheres, each enclosed in an organic envelope or diffuse mantle (variously described as mineral "ghosts" [72,73]. Each microsphere contains calcium phosphate in filaments of fixed diameter (5 nm) and variable length, which appear to be restricted by an organic framework of molecular dimensions. With the wider availability of reliable antibodies, some of the biochemically recognised but topographically and developmentally uncertain noncollagenous organic substances and adhesive proteins were related by Carter et al. [19] to the extracellular colonies of calcified microsphere "organelles". These include fibronectin, which encapsulates the microspheres in a manner which seems to confirm the nature of the microsphere as a calcified structure and not a random precipitate. Osteocalcin, sialoprotein, osteonectin, carbohydrates and lipids are all present within the domain boundaries, within the microspheres or between the microspheres and the domain boundaries. Osteopontin is a phosphorylated sialoprotein with an adhesive RGDS sequence, calcium binding sites and an affinity for bone mineral and cell attachment [74]. Moreover, osteocalcin has been described by G. Karsenty (ICRM, Montreal) as a "master regulator" hormone, its decline in the blood apparently associated with broad organellar senescence. In contrast with the immunofluorescence of collagen type I, FITC-labelled antibody, the microspheres appear in a dark profile [69], while the obverse is the case with fibronectin and osteocalcin when their integrity is found to persist in dense cortical as well as immature bone, contrary to the early assumption that microspheres are merely transitory features.

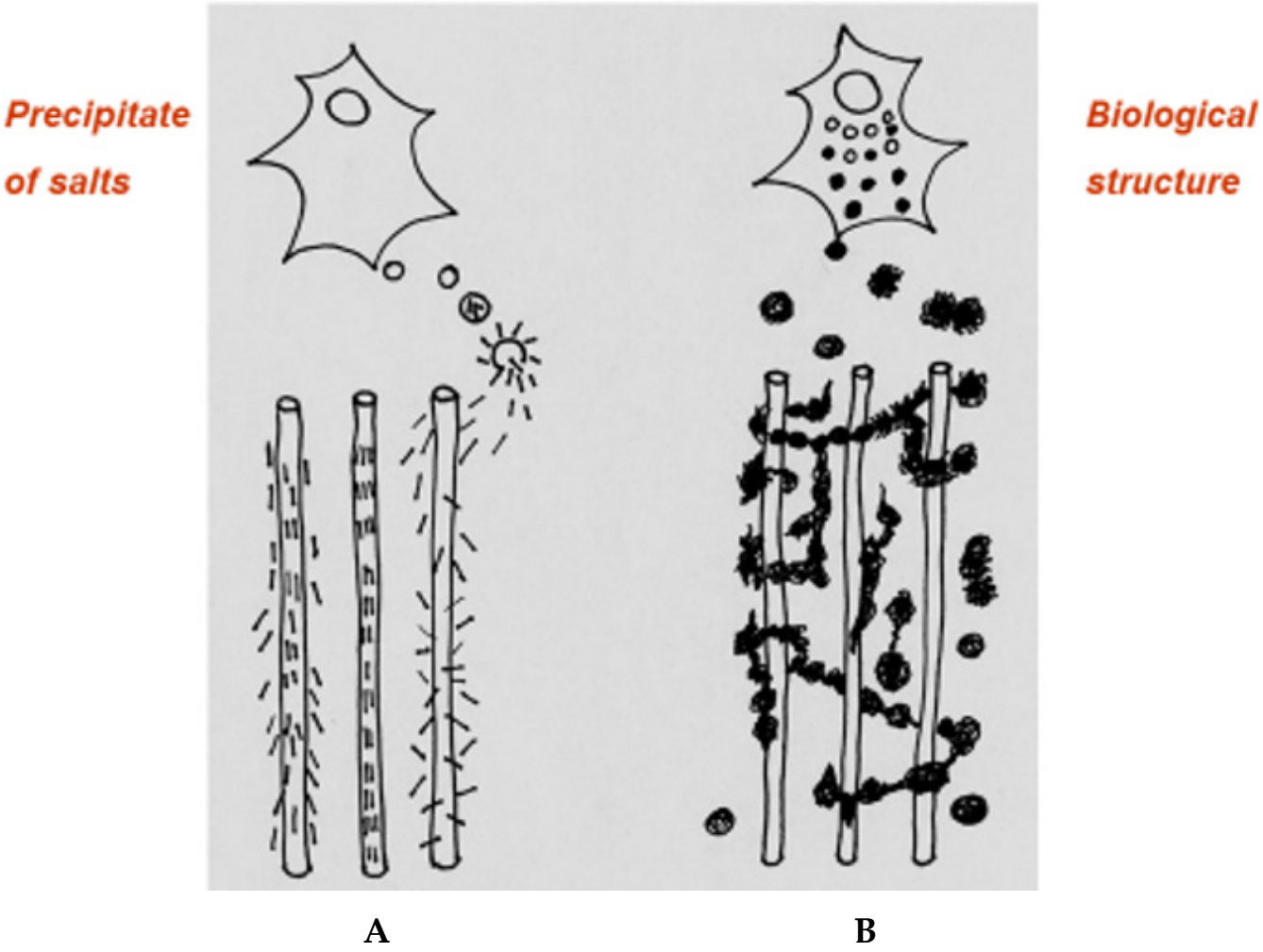


**Figure 10.** Diagram summarising divergent views of bone mineral: (**A**) as an extracellular collagen-dependent precipitate, subject to CRYSTAL FRACTURE microdamage; (**B**) as a cell-directed particulate fabrication, subject to PARTICLE SLIP microdamage. Archive image [27].

Collectively, they integrate into mosaic-like domains (10–30 μm) of indigenous histochemistry, e.g., osteocalcin (Shahtaheri [75,76]), variable lipid (most prominent at the calcification front), the Golgi-concentrated bone sialoprotein of Bianco et al. [72] and with osteopontin (specifically indicative of remodelling). Also included are hydrolytic enzymes, e.g., intermittent carbonic anhydrase activity and acid phosphatase [58,77,78]), though not alkaline phosphatase, which is associated with earlier pre-calcification osteoblastic activity [59]. At the same time, they stain positive for RNA and for the Gram microbe stain, and they have a powerful affinity for tetracycline antibiotic with which they form a stable fluorescent complex, which is the basis for their application as a reliable tissue-time marker of calcification dynamics [79,80]. Finally, contributing to an organelle-like modality is a tenuous outer lipid layer and an inner modicum of carbonate and silicon together with variable amounts of Mg, Al, Fe, Na, K, Cl, Bo, Sr tempering by trace element "doping" the inorganic phase from a less brittle, fatigue-prone state to one that is more stress compliant. Some trace elements arrive by chance contamination (e.g., Sr from weaponry, Fe from cooking vessels and Al from kidney dialysis).

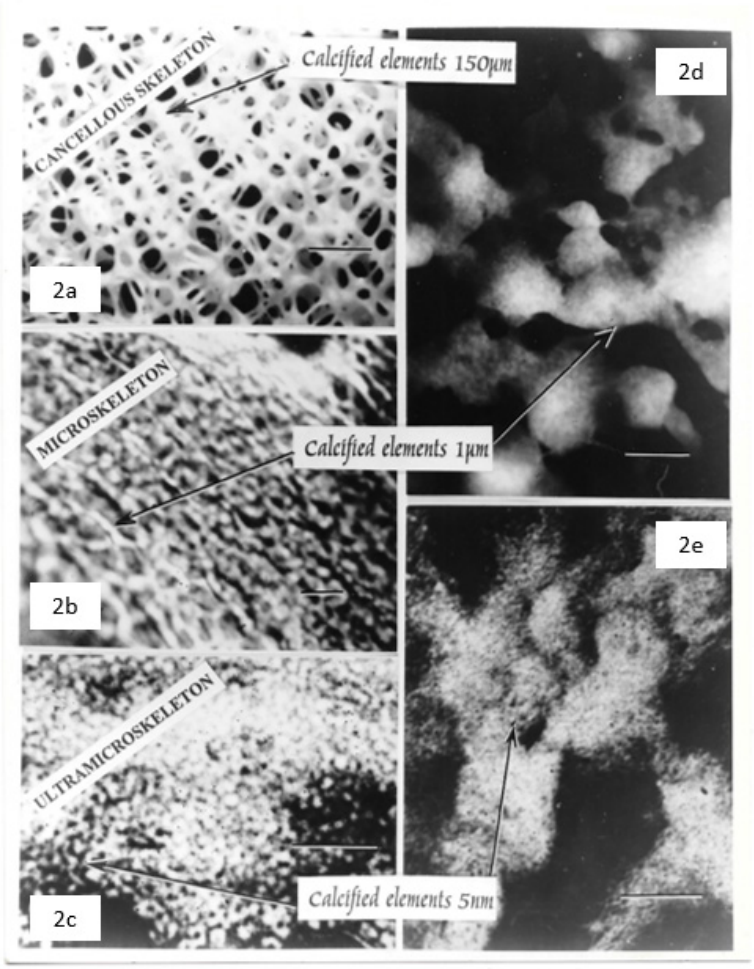


**Figure 11.** Illustrating the hierarchical bone mineral triad (mineral white, background black) of the cancellous skeleton (**2a**), microskeleton (**2b**), and ultramicroskeleton (**2c**). Integral to each trabecula (arrowed) of the cancellous skeleton is a microskeleton (1 μm gauge, arrowed) of micro-trabeculae composed of bridged assemblies of calcified microspheres (detail, **2d**). Integral to the microskeleton is an ultramicroskeleton (5 nm gauge, arrowed) of nano-trabeculae (detail, **2e**). Preparation: (**2a**) light microscope, defatted vertebra, 3 mm thick slice, scale bar, 1500 μm; (**2b**) polarised light microscope, iliac crest, 3 μm thick plastic-embedded section, von Kossa stain, scale bar 5 μm; (**2c**) transmission electron microscope, ultrathin section, mouse calvarium, potassium permanganate stain, scale bar 0.1 μm; (**2d**), transmission electron microscope, tetracycline stained mouse calvarium; (**2e**), as for (2**c**), scale bar 1 μm. Adapted from [27] 2003 and [58] 1980.

In sites that are primarily protective in function and adynamic, for example, fish scales of acellular bone, the calcified microspheres tend to remain uncoupled and less deformed than those exposed to stress where they align, interlink and compress for maximum resilience as ultrastructural struts and stays. Regional variation in average microsphere size will influence hydrogen bonding and fluid flow. In addition, it is an indigenous autoclastic mechanism characterised by local matrix hydrolysis, disintegration and fragment dispersal and is generally unencumbered by the time constraints imposed by osteoclastic recruitment and resorption [77,81]. This indigenous catabolic property acts as a functional "crumple zone" [see later] of rapid excess energy absorption. Disseminated fragments may regroup by callus formation into irregularly composite trabeculae, distinguishable by their disarray in polarised light in contrast to the orderly integration of lamellar remodelling units (Figure 12).

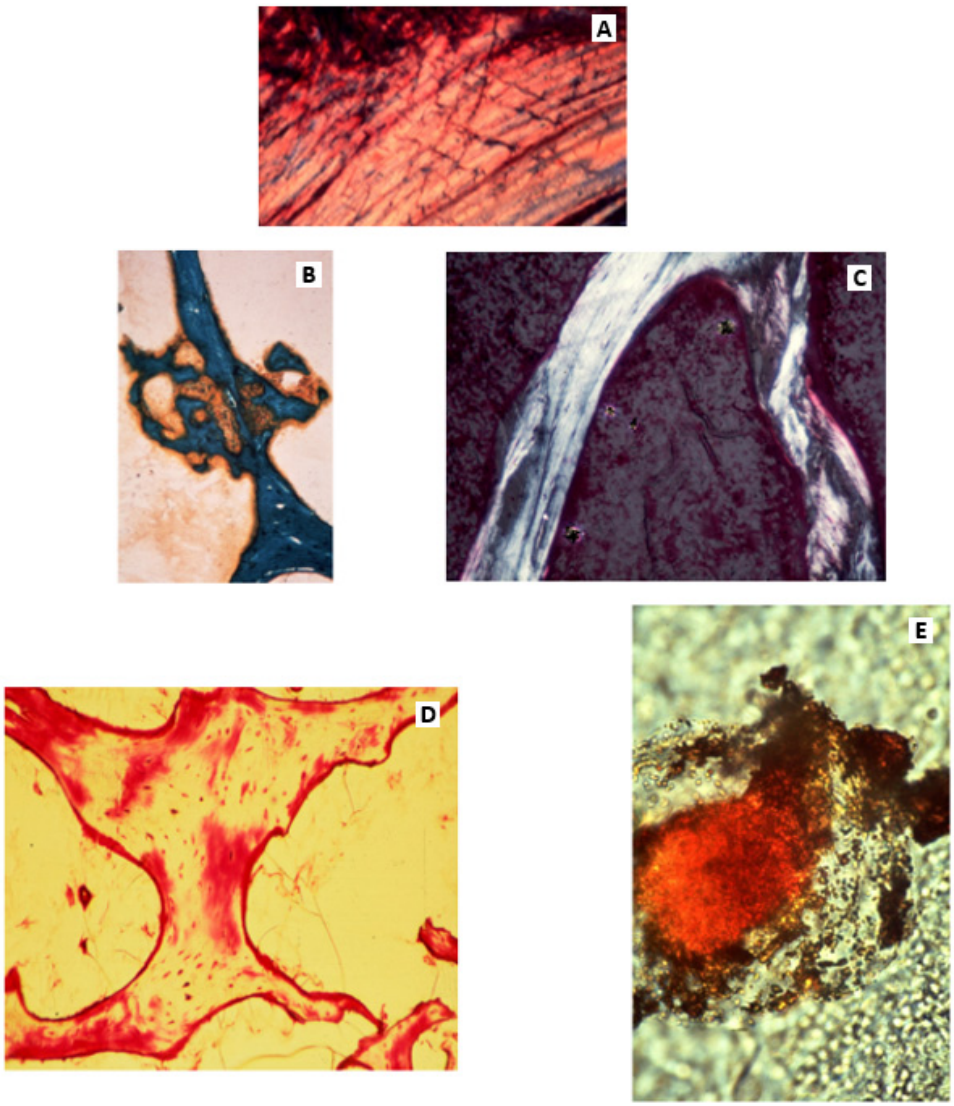


**Figure 12.** Showing aspects of microdamage. (**A**) Lamellar bone with cross-hatched microfissures in polarised light. (**B**) Microcallus repair of a fractured vertical trabecula, plain light. (**C**) A pair of trabeculae, one regularly lamellated, the other a mosaic of irregular fragments, polarised light. (**D**) Red fuchsin-stained trabecular areas of matrix permeability, i.e., "leakiness", plain light. (**E**) Trabecular "autoclasis" is when intrinsically calcified microspheres (about 1 micron diameter) are released into the marrow space [27].

Isolation of calcified microspheres: At formation sites, the calcified microspheres invest the collagenous matrix with their textural granularity before becoming confluent and vanishing from sight, which would seem to spell the end of them (other than a tendency to linger for longer in osteomalacia). However, boundaries are not lost with compaction but are merely deformed, as can be demonstrated by their restitution upon extraction as intact, rounded objects from even the densest cortical material [70]. Microspheres can be isolated in quantity to study their composition individually (Figure 13). To do this, the established digestion and density fractionation methods described in the literature (notably Ali et al. [82] to separate matrix vesicles have been modified to obtain the dense material. Isolation methods include density fractionation of freeze-dried or wet-milled, collagenase-treated bone; hydrazine, hydrolytic enzyme digestion (including collagenase, trypsin, papain, and that of the activities of soil fungi and the carnivorous digestive tract), pyrolysis followed by crushing, or by controlled etching in sodium hydroxide or potassium citrate, each of which preferentially splits the bridges [70]. In polarised light,

the majority of microspheres are non-birefringent but become birefringent in increasing numbers after exposure to absolute alcohol or incineration. When microsphere isolation is followed by decalcification (and also if sections are decalcified post- rather than pre-microtomy), aggregates of organic mineral "ghosts" of similar microsphere size remain to be differentially stained in the manifestation of a former calcified state. An additional feature, after enzyme isolation and mild potassium citrate decalcification, are a few microsphere "ghosts" attached to fine strands (0.5 μm thick) of unidentified composition and uncertain significance; a speculative identity is the calcium-binding proteoglycan of De Bernard et al. [83] or the nebulous remnants of Sharpey's fibre arrays.

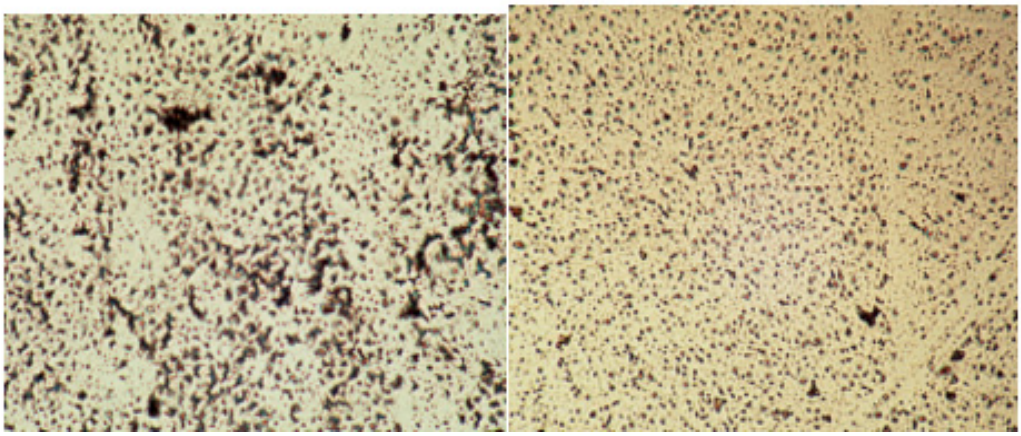

**A** **B**

**Figure 13.** Calcified microsphere populations isolated by density fractionation. (**A**) Micron-sized particles, mainly interlinked into bridged assemblies. (**B**) Micron-sized particles, mainly dispersed individually [70]. Archive image.

Irrespective of whether intact mouse calvarium or sliced ox tibia is used, the dense fraction of the extract is a pellet containing myriads of calcified microspheres for future analysis, but commonly discarded by others in favour of the lighter membranous, matrix vesicle-containing fractions (Ali and Sajdera [82]). At the same time, a less usual, natural approach to particulate isolation is brought about by exposure to the weathering attrition of millennia and preserved in the fragmented and fossilised skeletal remains that comprise the geo-biological sedimentary deposits of Khourigba and Senegal phosphorite and mined as fertiliser [16].

If the calcified microsphere population described constitutes the major, if not the entire, mineral component of bone, the general invisibility of these objects has to be explained. A number of factors appear to be responsible. Firstly, the nature, accessibility and distribution of bone salt at sites of formation may be altered by customary preparative procedures. Secondly, there is the almost universal predominance of analysing electrons over optical microscopy in determining the mineral/matrix relationship and the attendant well-documented problems of mineral solubility, stain-induced changes and ion transfer in the electron beam [84]. Thirdly is the considerable compression of the microspheres, which takes place as rising numbers compact, lose water and shrink, causing their domain boundaries to be masked and creating a deceptively homogeneous composition. Fourthly, there is the distortion of the spheres by mechanical stress along the axes of the matrix collagen fibres, producing an alignment between mineral and collagen commonly attributed to crystal epitaxy. However, microsphere size and shape are rapidly restored when rehydration follows the removal of in situ pressures either by partial demineralisation (chemical or pathological, [58]) or after biochemical or mechanical separation and density fractionation of the isolated microspheres. Fifthly, microspheres passing along attenuated cell processes may, in section, be mistaken for membrane-bound calcified matrix vesicles. While the concentration of submicroscopic matrix vesicles at sites of calcification has been

widely reported, doubts inevitably persist concerning their separation from the network of cell processes in the region and the capacity of all cells for exocytosis for a diversity of excretory, secretory and signalling purposes. Also, they generally contain alkaline phosphatase, which dissociates them directly from the mineralisation event and indicates a prior matrix preparatory role [59].

### *2.5. Cancellous Ultramicroskeleton (5 nm Gauge): Defined by Calcified Filamentous Clusters*

It may be a coincidence that microspheres of poorly crystallised hydroxyapatite, 1 μm in diameter and closely resembling those in bone, should equip the silt-burrowing protozoan *S. ambiguum* with its optional intracellular musculoskeletal system [37,43]. Similarly, it may be coincidental that there is a microbe (Figure 14) which is itself a microsphere calcified with phosphate via silicon [85,86] such that the skeletal particles of the prokaryote *Corynebacterium matruchotii* (previously named *Bacterionema matruchotii)* is a common oral isolate described as a single cell model for biological calcification (Linton et al. [87,88]). On the other hand, this organism seems to constitute a prokaryote link to bone minerals in terms of common factors that include motility, reproduction, colonial behaviour, symbiosis and gene expression, such that calcium phosphate microspheres are perhaps archetypal organelles sharing a prokaryote history of independence with the chloroplast, mitochondrion and centriole.

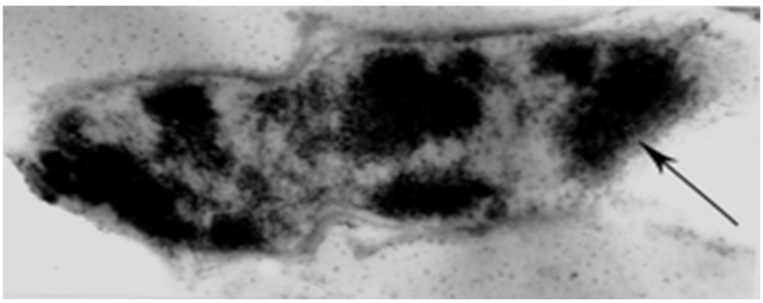

**Figure 14.** Bone mineral and bacterial calcification. Irregular electron-dense intracellular mineral microspheres calcified with phosphate (arrowed) assembled within the common oral bacterium *Corynebacterium matruchotii.* After Ennever and Creamer [85].

Calcification, silicification and a microbial model: Clinical attention has, for some time, included a functional association between bone mineral density and silicon (amongst the highest trace elements in human intake). One explanation for the apparently positive effect is a reduction in the biochemical deterioration of glycosaminoglycans and collagen in ageing connective tissues, together with an apparent affinity of silicon for the most metabolically active cells [86] and with less calcification in silicon deficiency. To investigate its possible role in biomineralogenesis, advanced optical (digital deconvolution and 3D fluorescent image rendering) and electron microscopy (EDX microanalysis and element mapping) have been applied to growing and calcifying microbial colonies. Here, calcium accumulates incrementally in dense intracellular microspherical objects as nanoparticles (5 nm), nanospheres (30–50 nm) and filamentous clusters (0.1–0.5 μm) with transitory Si content evident. With colony development (7–28 days), the P content increased from 5–60% while Si was displaced from 60–5% with a strong relationship between calcified object number and Si supplementation. The calcified objects (also positive for Mg) were extruded in bubble-like chains to coat the cell surface with discrete mineral particles. It was concluded that the orthopaedic activity of Si may derive from its special property to facilitate calcium phosphorylation (possibly via carbonate) in biological systems, recapitulating an ancient and conserved bacterial cycle of calcification via silicification [87,88]. It may be to these archaic roots that the clinical benefit of silicon in implantology is as fillers and coatings for prostheses and therapeutically for osteoporosis. The location of the mineral initiation step in the bacterial cell may derive from a fundamental organic cell-to-inorganic bone salt

interdependency of long duration, with silicon as the geobiological precursor of a commonality between invertebrate calcification and silicification via Golgi-formed silicon granules.

The inorganic nanoskeletal network; PARTICLE SLIP or CRYSTAL FRACTURE: The intra-particulate ultrastructural composition may vary in detail depending on the nature of the stress impacting the Golgi apparatus. For example, in silt-burrowing *S. ambiguum*, each microsphere encloses electron-dense, beaded filaments which typically radiate from the perimeter to the centre in an arrangement that differs from the more random coiled clusters of indeterminate length characterising vertebrate bone. The sinuous filaments, 5 nm thick, constitute the reticulated appearance of "nano-trabeculae" (Figure 11) as they are frequently laterally cross-linked. They commence within the "simple", non-membranous organic envelope (i.e., "ghost") of the microsphere, where they bear some resemblance to the "islands of crystallites" reported in calcified cartilage and usually in relation to either membrane-bound vesicles [82] or specific collagen sites [89]. However, the electron density of their mineral content varies along their length [43,54], and a beaded, 5 nm periodicity is commonplace, with matching diminutive organic "ghost" containers attributed to a protein-polysaccharide complex [73]. On exposure to robust chemicals, they tend to transfigure into uniform, needle-shaped "crystallites" some of which fuse laterally into striated plates and foreshorten into regular segments (Figure 15).

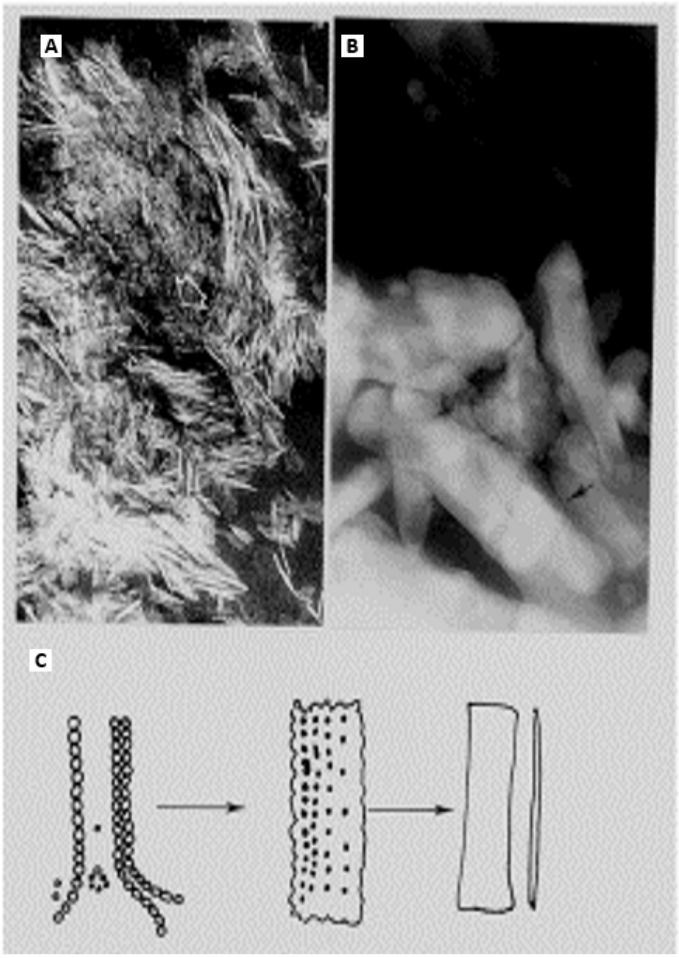


**Figure 15.** Showing (**A**) the filamentous ultrastructure of bone mineral (white, i.e., negative image) and (**B**) fusion of the beaded nanofilaments (5 nm diameter) into fenestrated plates and crystals. Preparation by D.H. Carter [6]. (**C**) drawings of the sequential transformation (arrowed) of the beaded nanofilaments from bone-like material for FLEXIBILITY/EXCHANGE, to the dentine-like property for COMPRESSION, to enamel-like for HARDNESS. Adapted from Ref [27]. 2003. Advances in Osteoporotic Fracture Management.

While the calcified filaments encircle a less dense centre, there are also skeins that extend into a tail-like projection, the combined configuration suggestive of a bridging ball-and-socket articulation interconnecting neighbouring microspheres, or alternatively a preliminary to a "budding" phenomenon of multiplication (Figure 16). Outside the cellular environment, the stability of the calcified microsphere increases as secondary bridges form between the primary filaments, creating a nano-spongiosa. This is evident in scanning electron micrographs [4,90] but is most reliably preserved in the material which has been "slam" frozen at −170 °C [6], followed by freeze substitution and EDAX analysis (energy dispersion X-ray microanalysis). Then, the rarity of needle-shaped "crystallites" in normal young bone seems inescapable, confirming the earlier observations of Arnott and Pautard [91,92]. Harnessed to the dynamic assembly of mineral microsphere "organelles" and their intrinsic complement of nanosphere chains (separable by freeze-milling into nanoparticles; Figure 17) [81] is a growing list of organic "ghosts" which haunt the sequential calcification event like interfering spectres at a feast. Their contribution apparently determines the stability of the micro- and nano-particulates and their graduated availability, or not, for fusion into amorphous nano-conjunction with progression towards microarchitectural struts and stays (especially evident in compression-resistant dentine) or laterally fused crystalline fenestrated plates [93]. Some "ghosts" are changed by their hydration state and by loose transitory bonds to function as lubricants and buffers. Accompanying are trace elements that may be in temporary storage or present as significant structural modulators of the inorganic phase, increasing compliance to stress and resilience against crystalline brittleness, microfracture, fatigue, and microdamage. In living bone, the dynamic nanoskeleton of inorganic ions is continually loading and unloading (unlike enamel) in response to homeostatic and mechanical stimuli; if that response is in balance, then the bone quality is optimal. In adynamic bone (e.g., fish scales), in contrast, the structural performance is more limited even though the mineral content may be unchanged.

In summary, a hierarchical Petrified Microbiome of considerable complexity is proposed (Figure 18), with biomaterial properties sensitive to both preparative manipulation and extraneous musculoskeletal forces. Periosteal Sharpey's fibres polarise the tensile and sexually diverse cancellous macroskeleton (postulated as microcosm I) and protect the stability of tendon/ligament insertion sites. The microskeletal Golgi-fabricated biomaterial (microcosm II) is assembled from complex containers of calcium phosphate (each as individually variable and responsive as the gross skeleton within which they function). Within their nanoskeleton (microcosm III), intrinsic proteins and elemental additives modulate amorphous/crystalline proportions, defining mechanisms for fatigue. The evidence suggests an evolved "Bone Mineral Microbiome" of ancient origin with biophysics that is yet to be addressed. While bone salt was grouped in 1926 by de Jong in the geological phosphorites (cited by Pautard [16]), it shares properties consistent with a "petrified prokaryote". In reaching a conclusion that is contrary to much-prevailing opinion about bone, we have applied a diversity of preparative methods over fifty years to produce our images and also have applied the methods of preparation used by others to produce their images in order to compare and explain the differences.

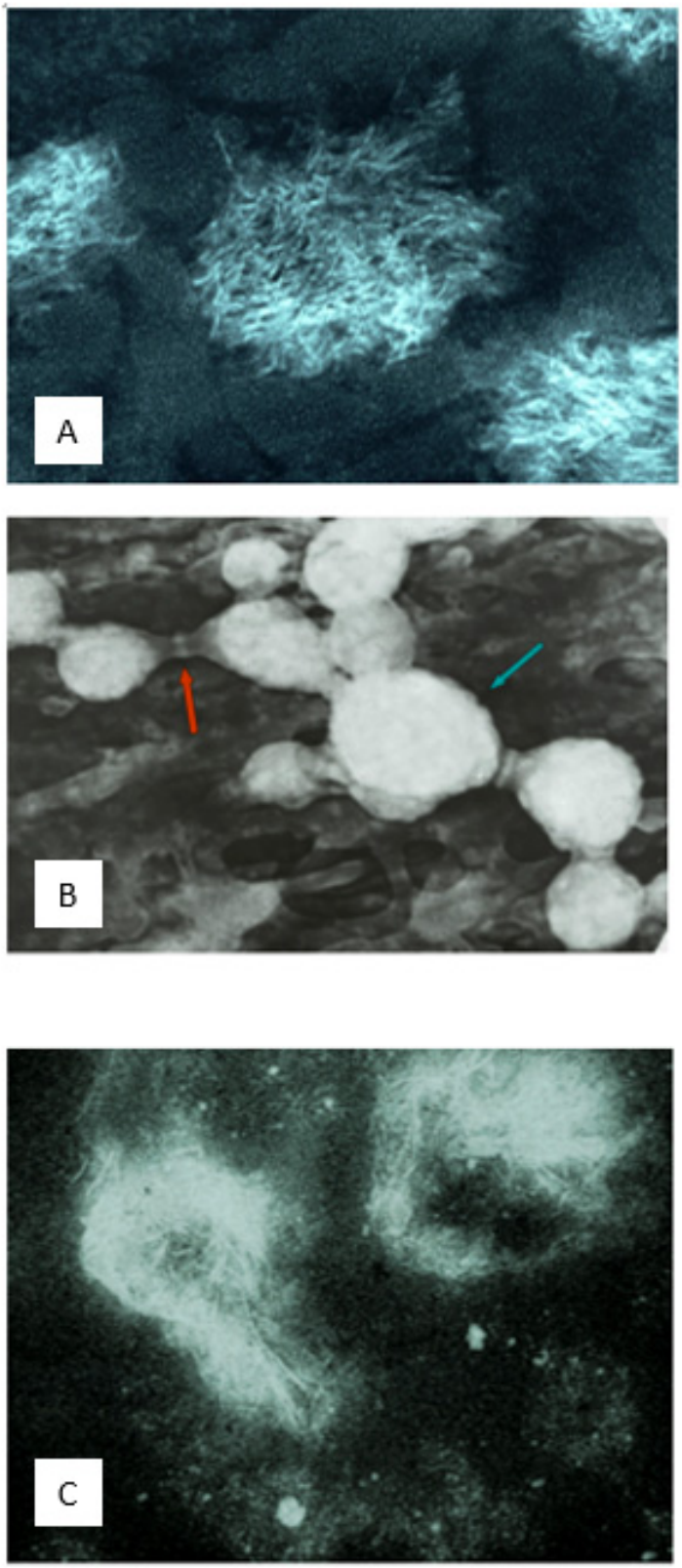


**Figure 16.** Calcified microspheres approximately 1 μm in diameter in ultrathin bone sections. (**A**) Trio of calcified microspheres showing their intrinsic composition of electron-dense filamentous clusters. Preparation DH Carter. (**B**) A complex assemblage of bridged (red arrow) calcified microspheres (blue arrow). (**C**) A pair of typical filamentous microspheres showing a common tail-like projection in one and a less dense centre in each. Silver-stained electron micrographs, negative images [54].

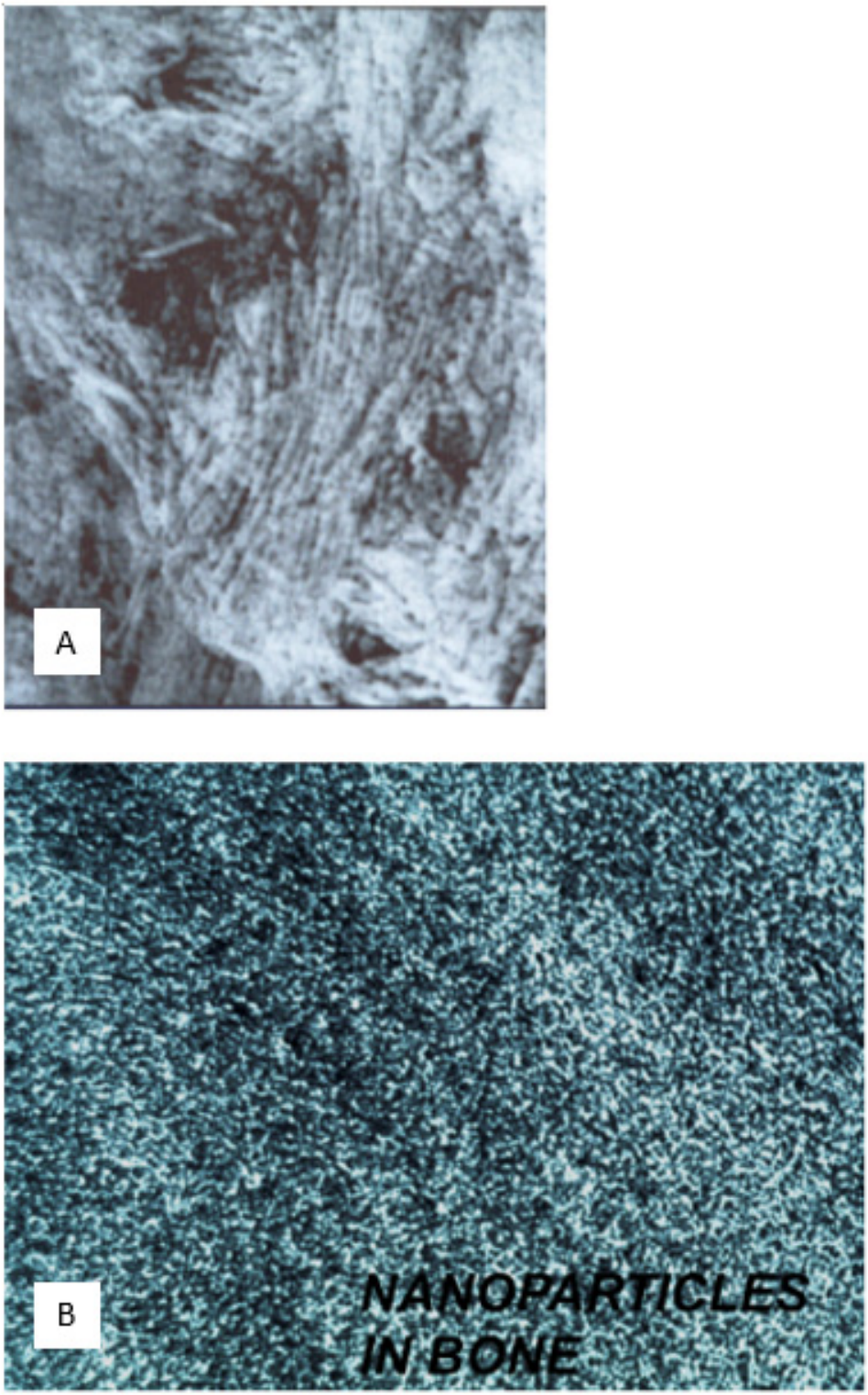


**Figure 17.** Slam frozen bone and chains of calcified nanoparticles. (**A**) In situ showing electron-dense beaded nanofilaments, 5 nm diameter, in adjacent compressed and deformed calcified microspheres (transmission electron microscope, mineral white as a negative image for better definition). (**B**) Released calcified nanoparticles (i.e., dark "beads" positive image) after isolation by freeze milling fractionation. Preparations by D. H. Carter [6].

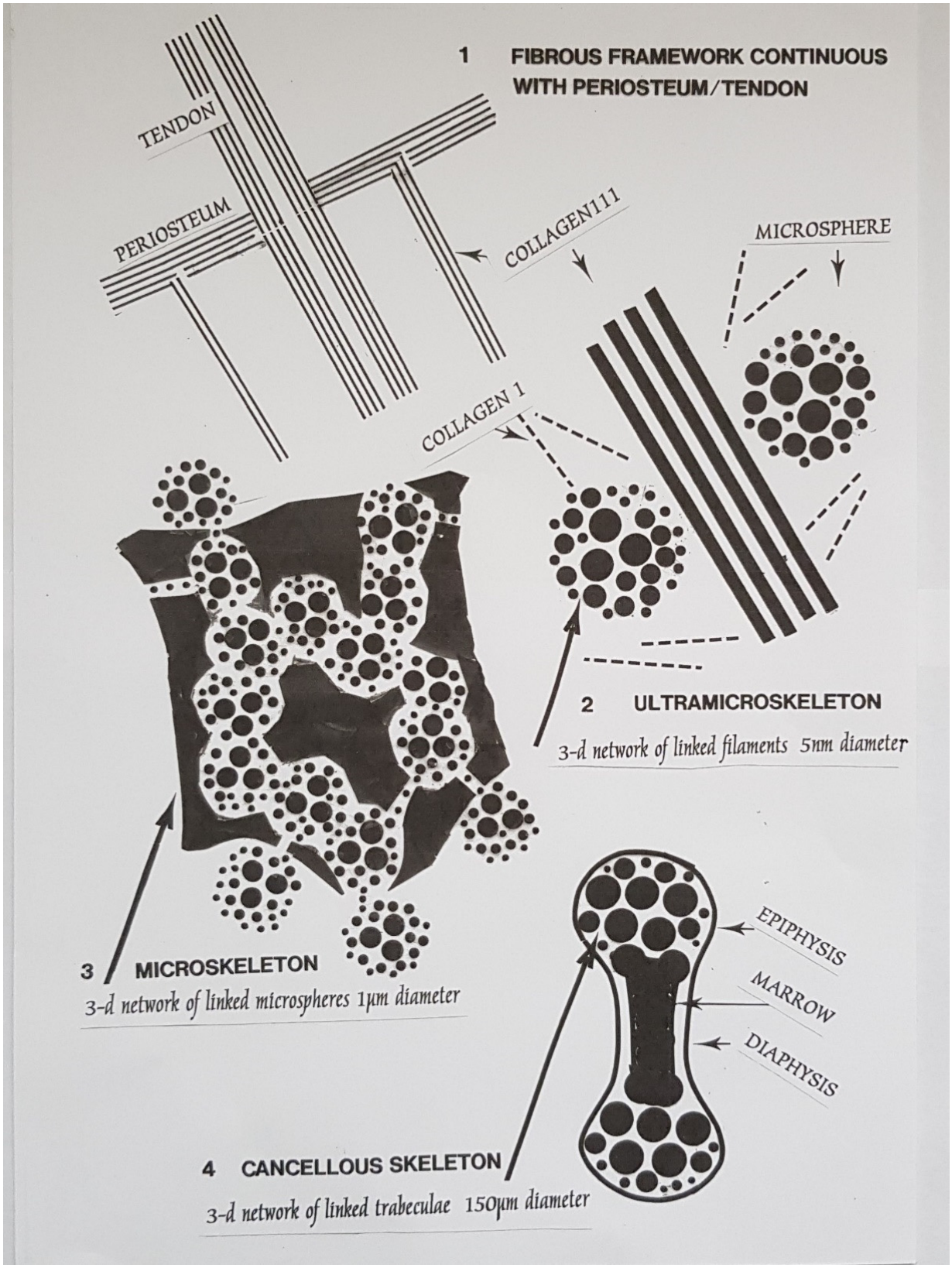


**Figure 18.** An early highly stylised diagram (Aaron, 1995) of the proposed biodynamic mineral phase of cancellous bone (mineral, white; background, black) suggesting a hierarchical calcified cancellous construct of macroskeleton, microskeleton, and ultramicroskeleton, permeated by intraosseous periosteal fibres. Data From [41,53].

## 3. PART II: Abnormalities in the Bone Mineral Microbiome: Morphogenesis of a Petrified Golgi-Fabrication Unfit for Purpose

Like microtubules, once witnessed calcified microspheres seem inescapable, both skeletally and as blood-born ectopic deposits. Bone mineral density is the product of millions of such deformable mineral microspheres which freely interrelate via covalent, ionic or hydrogen bonding and may be modulated in health and disease by intrinsic and extraneous factors (carbonate, pyrophosphate, fluoride, attachments to lipids, non-collagenous proteins, defective collagen fibrillogenesis, linkage hydrolysis). Clinical conditions arising from abnormal mineral metabolism often provide histological insight that is not otherwise evident.

It is suggested that the cancellous macroskeleton, microskeleton and ultramicroskeleton are also nominally microcosms I, II and III.

(1a) Periostal portal: altered Sharpey's fibre transduction and force perception.
(1b) Cancellous macroskeleton, i.e., microcosm I: trabecular atrophy or hypertrophy.
(2a) Osteocytes: abnormal Golgi body calcified microsphere fabrication.
(2b) Cancellous microskeleton, i.e., microcosm II: abnormal calcified microspheres.
(3) Cancellous ultramicroskeleton, i.e., microcosm III: filamentous transmutation.

### *3.1. Periosteal Portal: Altered Force Perception and Transduction*

The youthful periosteum varies in fibrillary strength and thickness according to inner osteoprogenitor cells and to bursts of enzyme activity stimulated by loading signals [94]. Sharpey fibre intraosseous insertion angles range from mainly oblique to vertical and maintain tendon/ligament anchorage stability.

Osteoporosis (i.e., a low-stress condition): The periosteum thins, and the main insertion angle of its Sharpey fibres declines towards the horizontal, while their fragmentation means fewer vertical insertions reach an equally attenuated endosteum. Scattered, fine mineral microparticles (1 μm) encroach and stiffen the system, undermining local stability by exposure to sub-periosteal and endosteal negative remodelling imbalance.

Osteoarthritis (i.e., a high-stress condition): Periosteal thinning is reversed, and while some Sharpey's fibres are attenuated and fragmented, a consolidated vertical fraction permeates to an endosteum, which is irregularly hyper- and hypertrophic. There is stiffening of the fibres by random, coarse mineral microparticles (about 2 μm), some densely compacted into sesamoid-like aggregates, contributing to irregular bouts of endosteal remodelling [95–97].

Oestrogen deficiency: The periosteum and Sharpey fibre arrays regress in synchrony with reduced musculoskeletal exchange and are consistent with reports of muscle atrophy at menopause. An ovariectomised rodent model (with or without the acceleration of calcium deprivation) [36] shows the effect is faster (within one month) in younger than older animals, with previously positive sites becoming negative as the Sharpey's fibres calcify, shorten and disappear in advance of matrix attrition [22,23].

Physical activity and microdamage: The well-exercised bone cortex was observed by Saino et al. [25] to be richer in collagen type III fibres, osteopontin and blood vessels, as well as maintaining optimal bone volume compared to less exercised bone. As intermediaries in musculoskeletal engagement, the differentially stimulated myotendinous Sharpey fibre insertions translate into microarchitectural modelling [95–97]. With exercise, intramembranous bone (rich in protective Sharpey's fibres) is subjected to the highest microstrain but does not remodel, while contiguous endochondral bone (devoid of Sharpey's fibres) engages in increased remodelling (when myotendinous exchange that is excessive, uniaxial or unstable may initiate osteoarthritis). In regions of substantial tendon and ligament anchorage, the priority of conserving long-term stability inhibits the remodelling of adjacent microdamage repair, predisposing to osteopenia in some and osteoarthritis in others. For example, excessive torsion in the Sharpey fibre anchorage of degenerate, collapsing discs may be responsible for vertebral epiphyseal rim erosion (as identified in archaeological specimens by M. Dobson, London; personal communication).

Dominant Sharpey fibre domains and fatigue microfissures: At articulation sites of maximum impact, the Sharpey fibre-rich domains are extensive and enclosed, as exemplified by the proximal femoral domain (rat model) and the adult mandible (porcine model). Their signal trajectory ends at the narrow, defined boundary, extraneous to which it is translated into matrix remodelling. With repetitive overuse, the shielded domain is at risk of irreparable fatigue microfissure accumulation. For example, overloaded periosteal Sharpey's fibres in Schlatter's Syndrome apparently relate to microfissure-accumulation in the over-stimulated knees of teenage footballers during the sensitive, signal-rich growth spurt (T. Maseide, Norway; personal communication).

Reconstructive osseointegration and "Embryomimetic Surgical Engineering": This orthopaedic intervention adopts Sharpey's fibre model of intramembranous bone regeneration together with the supportive microenvironmental principles of tensegrity to correct complex maxillofacial abnormalities. The basic science is applied to reverse-engineer the self-assembling morphogenesis of the foetal facial skeleton to reproduce a durable, bone-forming construct in an "embryomimetic" innovation pioneered by orthopaedic surgeon M. Chin, San Francisco [98].

Fibrous dysplasia and Sharpey's fibres: This pathology illustrates the essential role of the organiser protein tenascin and its macromolecular adhesive RGD sequence by omission. Its normal regular beaded pattern is integral to the Sharpey's fibres, which form the polarised primary scaffold for intramembranous bone formation; in the absence of tenascin from the Sharpey's fibres, the new trabeculae remain disorganised and immature [19].

### *3.2. Cancellous Macroskeletal (i.e., Microcosm I): Trabecular Atrophy and Hypertrophy*

The 20% of cancellous bone is especially reactive because of its expansive surface area for exchange. Here, a positive remodelling imbalance in the dominant arm of the professional tennis player can add 30% more bone mass. In contrast, a negative imbalance following paralysis and immobility may remove 60% within six months, while keen cyclists traditionally develop "good legs and bad backs". Factors increasing fracture-susceptibility are diverse, ranging from steroid therapy to space travel, while excessive resilience is shown by the South African Bantu.

Sex-related trabecular disconnection: The pattern of age-related cancellous loss differs substantially between the sexes. In ageing men (and steroid-induced osteoporosis in both sexes [99]), decreased bone formation results in widespread trabecular thinning with comparatively minor loss in trabecular number. In ageing women conversely (and in hypogonadal osteoporosis in both sexes), the trabecular thickness is little changed, while increased bone resorption causes a decline in trabecular number, significantly disrupting network integrity. The replacement of lost bars is more problematic than the consolidation of attenuated ones [99], and the consequence is trabecular network segmentation and weakness disproportionate to the amount of tissue lost (hormone replacement therapy provides some protection). Fluoride maintains bone mass via increased trabecular thickness; however, due to the deposition of osteoclast-inhibiting fluorapatite, turnover is poor, such that fatigue microdamage proliferates and fracture risk remains high (i.e., good quantity, poor "quality" [27]). Bisphosphonates such as alendronate are an alternative therapy to fluoride, with reports of fracture risk reduced by 50% in a single year, although the corresponding rise in vertebral bone mineral density is apparently only a modest 4%. An explanation for this success may be the cancellous microarchitectural protection from hypogonadal trabecular disconnection provided by alendronate and found by Hordon, Itoda et al. [35] to be significant in the conservation of the thoracic spine of an ovariectomised animal model.

Pregnancy-related trabecular disconnection (c.f., menopause): The trabecular modulation with increased random disconnection observed during the gestation period in pregnant women [76,100,101] is not the disadvantage it may seem; rather, it facilitates anabolic exchange while maintaining structural strength. In contrast, in postmenopausal women, the trabecular disconnection is not random but clustered in hotspots. It is a targeted, transaxial

catabolic reaction to an altered tensile and hormonal environment, an outcome of which are predestined "crumple zones" of deformation, which are rare in men [102].

Stress-related disconnection maps and floating segments: The contrasting conditions of osteoporosis (i.e., low stress, fracture-prone) and osteoarthritis (i.e., high stress, non-fracture) provide a convenient comparative tool [103]. In the low-stress osteoporotic female hip and spine, trabecular disconnection is not random but is clustered in "hotspots"; they multiply within predictable "hotspots" coincident with axes of tension [34,68], ultimately releasing "floating" cancellous segments into the marrow space [102]. In osteoporotic males, both disconnection and aggregation are less, with a general tendency to occur proximal to the vertebral endplates [68]. In high-stress osteoarthritis, the disconnections in women are equally as high as in osteoporosis, the essential difference being that their weakening effect is dissipated by their wide and random dispersal [103].

Trabecular reconnection: A biological pathway for trabecular regeneration de novo in the healthy, intact, mature skeleton is unclear, although there are novel avenues for consideration. (i) A pathological directive might emulate the positive sequence in Paget's disease whereby trabecular thickening by osteoblasts stimulates intratrabecular osteoclastic tunnelling to alleviate the centrally mounting cell hypoxia. The expanding channels indirectly transform the previous coarsening into a finer interconnected cancellous complex. (ii) An embryogenetic directive might emulate de novo trabecular generation on the primary scaffold of periosteal/endosteal fibres, such as that taking place locally after cancellous bone biopsy ablation, in response to which the insulted endosteum sprouts polarised Sharpey's fibres into the marrow space as a foundation for new replacement trabeculae. The process recapitulates trabecular generation in the human femoral anlagen where primary trabeculae arise either by endochondral ossification as fibronectin-rich mineral microspheres colonising collagen type II cartilaginous remnants or by intramembranous ossification when the calcified microspheres surround the tenascin-rich, collagen type III scaffold. Throughout development, the two trabecular types (endochondral and intramembranous) are physically separated by an intervening barrier of compressed fibroblast-like cells on a narrow ribbon of calcified cartilage [26,69], which separates form/function to opposite sides of the divide.

Trabecular disconnection, osteopenia and atraumatic autoclasis: Episodes of discrete trabecular fragmentation and particulate dispersal may facilitate osteopenic trabecular disconnection commencing with a localised increased matrix permeability (i.e., leakiness to tetracycline stain), followed by accumulating microfissures and progression to discrete clustered fragments in the marrow space. This sequential process of self-destruction named autoclasis (Figure 12E) may be summarised as (i) a mechanism of trabecular fragmentation and loss, which is separate from the cellular processes regarded as the principal agents of resorption and calcium exchange; (ii) occasionally reversed by initiating callus-related adhesion of the fragments (perhaps by growth factor release) into composite trabecula restitution evident using polarisation optics; (iii) an act of ablation due to indigenous, acellular hydrolytic digestion by enzymes including acid phosphatase and carbonic anhydrase [77] and possibly instrumental in atraumatic cross-strut atrophy following the apparent post-menopausal withdrawal of force-conducting Sharpey's fibres prior to bone loss.

Trabecular disconnection, osteoarthritic bone marrow lesions (BML) and traumatic "crumple zones": Osteoarthritic bone marrow lesions are subchondral single or multiple rounded sites (<15 mm diameter) of initially fibro-vascular, fatty-replacement tissue in response to abnormal or unaccustomed force transmission by denuded joint cartilage, impacting upon locations of trabecular disconnection and weakness. They may be summarised as (i) cyclically combining outer sclerosis and inner rarefaction with nascent, miniature radiating trabeculae polarised by attendant Sharpey's fibre arrays, a sequential conjunction resembling normal, spontaneous intramembranous repair by the endosteum following bone biopsy trauma; (ii) microcosms of ablation in osteoarthritis (with the prospect of wider skeletal implications for cataclysmic containment elsewhere), such that the cycle of trauma

within the discrete BML is the biological equivalent of strategic, energy-buffering, mechanical "crumple" zones [102] which may be widespread as a damage-limitation device.

### *3.3. Cancellous Microskeleton (i.e., Microcosm II): Altered Osteocyte Cohorts and Golgi Body Microsphere Fabrication*

Factors contributing to microskeletal behaviour, other than supplies of calcium phosphate at the right time and place, are poorly defined, the significance of the noncollagenous structural proteins is uncertain, and any direct action some of the vitamins, hormones and cytokines affecting bone may have on the performance of the Golgi apparatus is unknown. A contributory factor may be that lost bone tissue tends to be replaced by a tide of adipocytes (as reported by P.J. Meunier, Lyons [104]) at the expense of displaced osteoprogenitor cells (investigated by M. Owen, Oxford).

Osteomalacia, the Golgi apparatus and seasonal variation: Osteomalacia is the result of a diminished calcification front, histologically characterised by the low uptake of tetracycline labelling or weak metachromasia in toluidine blue stain (reported by P. Bordier, Paris). Unmineralised osteoid tissue accumulates at sites of bone formation in vitamin D deficiency syndrome; this is most evident in renal osteodystrophy and the inability of the kidney to make one of the active vitamin D metabolites. Less widely recognised than incipient childhood rickets is a covert susceptibility to mild osteomalacia in the elderly population of the UK due to an inadequate diet and infrequent skin exposure to sunlight. The deficiency exposes the Golgi apparatus and microskeleton to a cyclic seasonal variation, better served during the long days of summer than in the dark deficiency of winter [105] when femoral fracture risk is augmented by mild osteomalacia superimposed upon age-related osteopenia. Climatic effects combined with ethnicity apparently also contribute to microskeletal vulnerability in younger groups during pregnancy when foetal rickets may accompany maternal osteomalacia.

The errant microskeleton: There are circumstances when the microskeleton migrates or relocates as a satellite assembly. For example, in ankylosing spondylitis, the disabling calcification of the vertebral ligaments stiffens the spine to immobility, while conversely, the similar calcification of the leg tendons by looped and bridged assemblies of microspheres ensures the mobility of the heavyweight turkey (Figure 19). Generally, it is the Golgi apparatus that directs a sporadic calcification process in typically soft tissues outside the usual remit of the mineral microsphere (indicating the cellular ubiquity of the particulate event). At the same time, properties and constituents may be functionally modulated as described by Al-Qtaitat [95]; for example, in the trachea are microparticles rich in carbonate, in this regard apparently resembling those in ear ossicles. In addition, individual micron-sized objects may be released into the circulating bloodstream to settle anywhere (as suggested by cases of calcifying aorta related to particulate release during decalcifying osteoporosis). With longevity, Golgi-directed discrimination between cell types apparently diminishes, perversely permitting soft tissues to harden (ectopic calcification) and hard ones to soften [49,96,97].

Stress, the osteocyte Golgi apparatus and microsphere size: In the low-stress condition osteoporosis, a poorly interconnected osteocyte syncytium contrasts with that in high-stress osteoarthritis, where cell processes are numerous and consistent with anticipated high mechano-transduction. Similarly, the syncytium cell volume is small in osteoporosis in contrast to the more capacious cytoplasmic volume in osteoarthritis, perhaps indirectly related to the degree of Golgi body activity. It follows that when field emission gun scanning electron micrography (FEGSEM) was applied by Linton et al. [103] to the human mineral articulation front ("tidemark") of the osteoporotic femur (with characteristic thick uncalcified and thin calcified cartilage layers, i.e., soft and pliant) the neighbouring chondrocytes were small and appeared hypotrophic. The under-stressed cells fabricated precursor nanospheres (30–50 nm) and mature microspheres that are abnormally small in osteoporosis (0.5–0.7 microns), constituting a fine-textured, smooth and compacted microskeletal tidemark [Figure 20]. Conversely, in osteoarthritis (with characteristic thin uncalcified and

thick calcified layers, i.e., hard and unyielding), the nearby chondrocytes appeared hypotrophic. The over-stressed cells fabricated precursor nanospheres (>100 nm) and mature microspheres that are abnormally large in osteoarthritis (0.5–4 microns), constituting a coarse-textured, uneven and irregularly dispersed microskeletal tidemark [103]. Although the particles fabricated by each Golgi apparatus are small in osteoporosis, they are not necessarily fewer in number. Such particulate textural differences will influence matrix interstitial fluid flow in a manner analogous to fluid flow in clay where the particulates are fine and compact and, in consequence, prone to slow water passage; in sand, they are coarse, and their settlement open and prone to rapid water passage. A particulate mix is best, and so may it be for the hydrodynamics of bone.




**Figure 19.** A collagen bundle in turkey leg tendon in polarised light shows bridged assemblies of calcified microspheres, each approximately 1 micron in diameter, and collectively provides a large bird with a powerful arrangement that is fit for biodynamic purposes. Permission from [95] 2004, A. Al-Qtaitat.

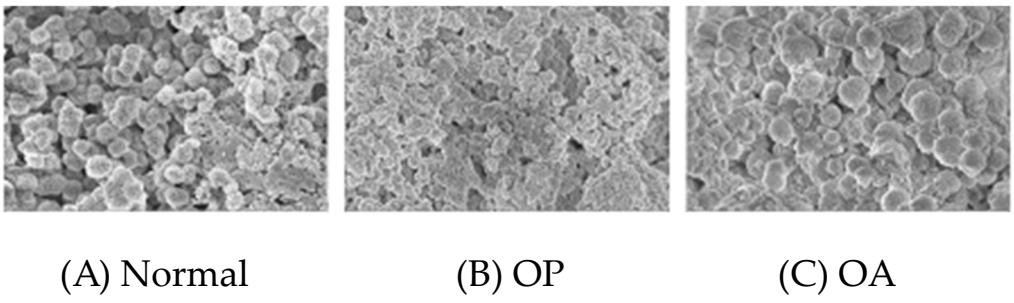


**Figure 20.** Field emission gun scanning electron micrographs (FEGSEM) showing a significant particulate size difference of matrix microsphere dimensions from normal in (**A**) to abnormal in (**B**) osteoporosis and (**C**) osteoarthritis. Preparation by K.M. Linton [103].

Microskeleton and trace elements: Si or Mg "doping" of the inorganic phase diminishes with age, potentially influencing its matrix dynamics. Digestion of the matrix by various means produces myriads of microspheres together with small numbers of rudimentary, precursor, low-contrast nanospherical objects. Their individual bioactivity may be modulated by small quantities of inorganic ions such as Si, Mg, Al, Na, Fe, K and S, their traces tending to decline with distance from the calcification front. A trend is suggested towards a poor Mg content within the OP microsphere substructure (Ca:P ratio 1.61) and a paucity of both Si and Mg in OA (Ca:P ratio 1.72) relative to a young adult reference and

also to a porcine model Ca:P ratio 1.58). Perhaps one-day treatment for a Si/Mg imbalance may aid elderly skeletal performance [103].

Microskeleton and particle slip: Because the mineral microparticles in bone are generally completely enshrouded by an organic envelope of uncertain composition with mineral "ghosts" regularly described (and evident after decalcification), they have no exposed surface from which to react, and any linkages formed are hydrogen bonds due to the presence of water. At a crucial point of water content, the hydrogen bonding is sufficiently powerful to safely support the activities and daily stresses placed on the bone (above and below this, the bonds are weak, and the particles are, therefore, more mobile). However, damage caused by repeated stresses can disrupt the hydrogen bonds, causing a "slip" of the particles [27]. At the micron level, the graduated scale of hydrogen bonding determined by the water content moderates extraneous pressure, ensuring that there is no fracture of the enrobed and noncrystalline microparticles, only slipping between the two. A high bone turnover optimises hydrogen bonding status, increasing strength and confining damage.

### *3.4. Cancellous Ultramicroskeleton (i.e., Microcosm III): Filamentous Clusters, Macromolecular Transmutation and Antigenicity*

Problems of microdamage for the orthopaedic surgeon and of turnover for the physician may be considered in relation to the dynamics of bacterial-sized clusters of nanometer beads. While the combination of calcified microspheres above constitutes an independent articulating microskeleton, it colonises the collagenous matrix, at the same time, interlocking skeins of collagen fibres into place for maximum strength; also interlocked are the filamentous skeins of nanometer beads, preventing structurally committed mineral from being indiscriminately available for free ionic metabolic exchange. The bone which fails to remodel or which is subject to sudden unaccustomed stress may become increasingly more crystalline and fatigue-prone, as exemplified by young and previously untrained soldiers who suffer "march" fractures (with occasional microcallus repair) not encountered in progressively exercised feet. Enamel, in contrast, differs from bone in that its mineral is exposed and highly crystalline; there is no water, therefore little hydrogen bonding and when stressed, it does not "slip" but displays crystal fracture (Figures 10 and 15; [27]). Such morphological transmutability adds a spectrum of immunological significance to bone salt which is of relevance to resorption.

Nanodamage, permeability and crystal fracture: Elements such as pyrophosphate and fluoride affect mineral amorphous/crystalline proportions, influencing "crystal fracture" as an underlying mechanism for ultramicroskeletal damage evident as little more than the regional permeability to mineral stains such as tetracycline of a normally impervious intact matrix, and resulting from unaccustomed repetitive motion, low density or excessive stress [81].

Nanodamage, geometric constructs and crystal fracture: There are circumstances of force exposure when bone may behave more like enamel. The differential removal of the enshrouding noncollagenous proteins from the nano-beads, freeing from suppression of their mineral modulation, facilitates the lateral fusion of the exposed slender filaments into crystal-like plates (for example, after hydrazine hydrate digestion to prepare anorganic bone). This format has only been observed so far in elderly subjects at compression-resistant locations, such as the femoral subchondral bone. Here, the filamentous ultramicroskeletal structure of deformed microspheres is evident in the youthful subchondral material. However, in the aged femur, the subchondral mineral nano-filaments may fuse into a diversity of geometric calcified constructs, sometimes fenestrated plates, sometimes featureless needles and rods, sometimes compression-resistant, highly orientated struts and stays (as in dentine). Even in low-stress OP, the microspheres may be confined to spaces between thin mineral rods and occasional mineral plates with few visible traces of a filamentous ultrastructure. In high-stress OA, branched rods and broad featureless plates are commonplace at this location, together with the deformation and fusion of the beaded filaments by axial

pressures within the matrix in diverse architectural configurations of compressed calcified assemblies [27].

Pyrophosphate, crystal fracture and the ank-gene mutant: An increased predisposition to crystal fracture may relate to the removal of enshrouding noncollagenous proteins and also to a deficiency in pyrophosphate, which regulates the degree of mineralisation and crystallinity, as indicated in the excessively calcified joints of the ank-gene mutant mouse where the extracellular matrix lacks its modulating influence. The condition is ameliorated by pyrophosphate drugs. Although bisphosphonates may have an unacceptable demineralising effect, they currently seem to be the most favourable fracture prophylaxis. An ideal drug would optimise the amorphous/crystalline mineral balance for maximum structural strength.

Bioimplant material and transmutability: The graduated transformation from a biomorphology to a geo-morphology is particularly evident en route in rigorously processed clinical bone mineral biomaterials [93] (deproteinated; heated to 300 °C to kill viruses; strong alkali treatment; defatted in organic solvents; dry-heat sterilised; dehydrated). Optimally prepared (low-temperature milling) human and bovine bone consist of 5 nm thick beaded filaments; in comparison, (i) deproteinated material typically consists of 50–80 nm wide plates, and (ii) a commercial bioimplant product (bovine) consists of 50–200 nm wide rhomboidal, plate-like forms or about 10 nm edgeways, with only minor traces of natural fenestrations and striations. The removal of the noncollagenous, mineral-bound proteins propels the beaded filaments along a physicochemical path towards rhomboidal plates (in the elderly, perhaps a hallmark of natural bone salt senescence).

Bioimplant material and antigenicity: Unlike the fine, filamentous mineral, the large plates are antigenic and (assuming accessibility) able to produce an inflammatory response, as demonstrated by their strong nonspecific affinity for immunoglobulins. Accompanying their unmasked antigenicity is an intrinsic yellow autofluorescence not shown by fresh material. The affinity of hydroxyapatite for many organic substances, including immunoglobulins, is well documented and may explain the nonspecific immunohistochemical staining of enamel. To cite DH Carter [93], "A merely superficial structural and chemical similarity between a biomaterial and its host tissue may be no guarantee of biocompatibility. The deproteinated bone mineral may provide a suitable surface for the apposition of new bone (like other nonbiological materials, e.g., titanium), but without appropriate organic masking and constraint, its exposed topography may be so 'noisy' with spurious signals that it no longer presents the highly selective morphological and biochemical motifs that mediate natural bone remodelling and healing, with pathological consequences". In this way, the inorganic phase of bone seems to be both morphologically and immunologically transmutable, and the natural ageing process combines progressive stiffness with rising immunological reactivity.

Anomalous traits and adsorption artefacts: A dependence upon the presence of silicon seems to be a molecular bone mineral hallmark, together with three other apparently anomalous traits [79,86]. Firstly, is their strong microbial gram-positive staining property (crystal violet/iodine staining of peptidoglycan; perhaps an echo of prokaryote-related ancestry, although not always specific, can stain collagen). Second, is the widely recognized binding of tetracycline to produce a fluorescent complex with bone salt so specific that it has become a histomorphometric tool for measuring bone formation dynamics (as well as identifying particles calcified with phosphate in otherwise soft tissues. Third, is a differential affinity for routine nucleic acid histological stains (methyl green/pyronin Y) showing a propensity for concentrated red RNA stain in microspheres at the discrete calcification front [79] and paler pink in the mature matrix beyond (with acellular bone from fish scales exhibiting the same phenomenon; D. Stoker, student, unpublished final year dissertation). Much of this widespread affinity between bone salt and RNA stain seems unlikely to be due to the physical presence of organic nucleic acid macromolecules. While it may, therefore, be an adsorption artefact, it may be a meaningful one, whereby a complementary, naturally occurring "microcrystalline" bone salt template for nucleic

acid is imprinted as a regular feature of the mineral surface. Of special relevance may be the attribution to the presence of parallel surface grooves on microcrystals of apatites (and possibly silicates), defining adsorptive and catalytic properties and a perfect fit for nucleosides, nucleotides and pyrophosphate. Related to this specific phenomenon is the separation according to the structural feature of amino acids in relation to their adsorption by a slurry of apatite crystals on thin-layer chromatography plates, properties postulated by the authors Burton and Neuman [106,107] as instrumental in the origin of life forms (also Taves and Reedy who had described adsorption of nucleosides, nucleotides pyrophosphate and amino acids by apatite crystals) and with a last word to Pautard [108–110] on his inorganic "Road from Rocks to Reason".

In summary, with regard to functional decline, the extracellular matrix components in receipt of a diversity of forces are (i) collagen (subject to erosion in low turnover, linkage hydrolysis, defective fibrillogenesis regulated by osteonectin; (ii) polysaccharides and glycosaminoglycans (inter-fibre polymers generally easily damaged and repaired; changed by their hydration state and by loose transitory bonds to serve as lubricants or buffers); (iii) mineral microspheres with independent biochemistry and implications of density, crystalline/amorphous states, regulation by carbonate, pyrophosphate, fluoride, and diverse attachments to lipids and noncollagenous proteins (bone sialoprotein, osteocalcin, osteopontin).

The proposed Bone Mineral Microbiome is subject to dysfunction with chance and circumstance at any level including: (i) permeating periosteal fibres that are atrophic, misaligned, calcified, incomplete or otherwise incoherent; (ii) a macroskeleton that is disconnected and disproportionately weakened by age, especially in women; (iii) a microskeleton of mineral particles the intrinsic morphology and biochemistry of which are influenced by signalling anomalies received by osteocyte Golgi bodies which in response fabricate within their cisternae organically enshrouded, calcified microspheres that are inherently substandard influencing mineral texture; (iv) an ultramicroskeleton (or nanoskeleton) of beaded filamentous clusters modulated by superficial or incorporated molecules (e.g., fluoride, carbonate, pyrophosphate increase or reduce crystallinity respectively) or deficient trace elements (e.g., Mg, Si, Zn, Al, Fe as "doping" agents modulating crystallinity), or the differential removal of enshrouding proteins ("crystal ghosts") allowing lateral fusion into crystal-like plates, exposing spurious antigenicity and shifting predisposition from particle slip to crystal fracture influencing biomaterial properties of microdamage and fragility.

Two insightful, stress-related diseases of the Bone Mineral Microbiome are low-stress osteoporosis and high-stress osteoarthritis. The first is a biomaterial of atrophic trabeculae, withdrawn periosteal Sharpey's fibre arrays, cancellous disconnection "hotspots" and the release of "floating segments" of little structural significance. In addition, is the limited dynamic perception of a diminished osteocyte syncytium, hypo-stimulated Golgi body cisternae fabricating microspheres (and precursor nanospheres) that are abnormally small, resulting in a microskeletal assemblage that is sub-optimally fine in texture, decreasing matrix fluid flow. The second is a biomaterial of hypertrophic trabeculae, expansive periosteal Sharpey's fibres, randomly aberrant cancellous disconnection and bone marrow lesions (BML) at sites of unbuffered high impact. In contrast, is the acute perception of a signal-sensitive, augmented osteocyte syncytium and hyper-stimulated Golgi body cisternae fabricating microspheres (and precursor nanospheres) that are abnormally large, resulting in a microskeletal assemblage that is abnormally coarse in texture, increasing matrix fluid flow. The evidence suggests that the colonisation of the collagenous matrix by the petrified microbiome may be dysfunctional at several levels, attributable to archaic, organelle-like objects deflected by primordial dynamics and adding a novel perspective to bone disease.

## 4. Conclusions

What is the nature of the proposed Bone Mineral Biosystem? There is much in the literature about the inorganic phase as a stoichiometric matter of collagen-dependent

precipitation (<0.1 micron) and slow epitactic growth into crystalline sheets. If correct, it leaves an unusual assortment of associated properties in need of an explanation, which features such as a sub-crystalline amorphous state (A. Posner, USA) and matrix vesicles (E. Bonucci, Italy) have previously sought to meet. It is suggested that a comprehensive answer may be found at the roots of biology in a unified web of diverse modalities as an evolved calcification legacy inherited from a stressed contractile protozoan and a cyclically silicified bacterium competing for depleting levels of phosphate in a stressful, primordial pool.

In particular, the bedrock stability of the most vulnerable regions of the vertebrate skeleton is determined by the efficiency of trabecular networks in conducting multiaxial extraneous forces across a sequential biomorphological system. It is dependent upon (i) the translation of force-recipient periosteal Sharpey's fibre networks and juxtaposed osteocyte cohorts into, (ii) the stimulation of Golgi-fabrication and the subsequent convoluted assemblage of organically enrobed, bridged and deformable microspheres calcified with phosphate/carbonate and each of organelle-like coherence that is finally, (iii) marshalled extracellularly into a polarized, bespoke compaction of modulating skeins of 5 nm filaments optimally aligned against force-generated microdamage. The integrated reticulations of the macro-, micro- and nano-skeletal systems may usefully be described as the hierarchical microcosms of a self-contained and force-discriminating "Bone Mineral Microbiome".

The seasonally variable and hormone-responsive populations of Golgi-fabricated micron-sized objects are organically enshrouded (bone sialoprotein, osteocalcin and post-remodelling osteopontin), immunologically transmutable, and harbour an independent biochemistry (indigenous carbonic anhydrase and hydrolytic enzymes, such as acid phosphatase released during the self-destructive process of autoclasis). Properties of form and dimension, interlinkage into chains and convoluted assemblies via tail-like projections, replication by budding, colonial habit into domains approximately 30–50 microns, together with intrinsic properties of Gram stain positivity, tetracycline antibiotic affinity and nucleic acid staining may be dismissed as material aberrations. On the other hand, they may facilitate microbe-like objects under extraneous pressure to progress on the road to backbones in the collective manner of a "petrified microbiome".

A "petrified microbiome" and protozoan beginnings? The evolutionary significance of the backbones of an otherwise undistinguished protozoan (*Spirostomum ambiguum*) was suggested by Pautard (1959, 1961; [11,110]). Since then, and with Golgi body bone mineral fabrication, it follows that chronic bone fragility may derive substructurally from an underperforming Golgi program imprinted on a transmutable apparatus to stiffen a delicate protozoan tunnelling through primordial silt after the pond water evaporates.

A "petrified microbiome" and prokaryote beginnings? Bacteria may predate the Golgi body (possibly vestigial like the mitochondrion, centriole, chloroplast) as suggested by the prokaryote-directed cyclic assembly in the oral bacterium (*Corynebacterium matruchotii*) of similar bone mineral microspheres and precursor nanospheres (40–250 nm) calcified with phosphate in a silicon-rich intermediary for the purpose of mechanical and metabolic advantage [87].

A "petrified microbiome" and pre-prokaryote beginnings? Precedent to this may be the emergence of a silicified primordial particle through an ancient geological portal whereby the omnipresence of silicon in bacterium, protozoan and osteocyte alike derives from its singular property of facilitating calcium phosphorylation via carbonate to protect and energize biological systems. In this way, some of the ancient sedimentary rocks of phosphorite contain the most intractable bone mineral remnants [16] and are mined as an invigorating plant fertilizer, metaphorically returning the bone "dust" to the roots of biology from whence it came.

The eukaryotic biosystems apparently evolved from the first prokaryote biosystems at a time 4500 million years ago, prior to which only minerals and simple molecules occupied the thin skin of an early planetary ball of molten iron. While we may be made from stardust, how the leap from one to the other was navigated remains uncertain.

At the very least, there is an assortment of properties to be explained. Few would deny the challenge of interpreting dynamic events from static images at a geobiological interface of exceedingly small dimensions between calcified objects and cells. Added to this is received advice concerning the impossibility of making dynamic predictions at the animate/inanimate frontier of bone, where the laws of inorganic chemistry are less applicable. The closest to reality may be a cohesion of several views, especially the prebiotic role assigned to hydroxyapatite crystals by W.F. Neuman [106,107]. At the same time, recognition of misleading mimicry across biology cannot be dismissed, and all may not be as it seems; for example, the bee orchid is still a flower even if it does look like a bee [49,79]. However, on the basis of a half-century of histological observation, I cannot escape the conclusion that the reclusive occupant of the expansive geo-biological mineral frontier is a small, petrified microsphere of understated complexity (Figures 21 and 22), fabricated by an entombed maternal Golgi apparatus to fulfil a compendium of extraneous metabolic and biomechanical demands; clues to our origins, as well as our social history, may lie in our bones.



**Figure 21.** A single calcified microsphere (approximately 1 μm diameter) from dentine (mineral white) showing variable density and internal ultrastructural complexity, whereby electron-dense beaded filaments (5 nm diameter) are interspersed with dense nanospheres (transmission electron microscope, as a negative image for better definition). With permission from Ref [97], 2007, A. Al-Qtaitat.



**Figure 22.** An early archival electron micrograph (circa 1974). Now reinterpreted as a population of electron-dense microspheres (each approximately 1 micron) apparently colonizing the extracellular matrix, dispersed singly and in looped assemblies, thereby binding collagen fibre bundles for added biodynamic strength. (Transmission electron microscope, positive image, i.e., mineral black).

Finally, with the benefit of five decades of national and international associations, another look has been taken at an old problem. While a proportion of the extensive calcification literature on the topic of bone microarchitecture and mineralisation is addressed, there is apparently little elsewhere connecting the periosteal Sharpey's fibre—Golgi body axis to the event, nor to the analogy of a "petrified microbiome" as witnessed by the accumulating reports above [1–110]. For that reason, and in acknowledgement of a comprehensive bone mineral "state-of-the-art", a representative selection of references from a number of established authors has been added [111–147]. Relative to their context, the first concern is *cancellous* microanatomy [111–117]; there follow the diverse opinions surrounding calcification with phosphate/carbonate as (i) an extracellular material conforming to the rules of apatite crystal epitaxy on matrix collagen fibres [118–125]; (ii) as a noncrystalline amorphous material [126,127]; (iii) extracellular commencement in matrix vesicles [128–131]; (iv) intracellular commencement within cytoplasmic vesicles [132,137], especially evident in invertebrates [50–52,138,139]; (v) origins within mitochondria [140,141]; (vi) origins in microbiology as a feature of calcifying bacteria [142] and of genetic association [143]; (vii) perhaps pertaining to the Golgi apparatus [144–147].

**Funding:** Support for my Bone Structural Biology Laboratory is gratefully acknowledged by the Medical Research Council for its initial inauguration in the Mineral Metabolism Unit, Leeds and its continuance beyond at the University of Leeds and in collaboration with Sheffield and Manchester Universities, together with grants enabling its longevity from Action Medical Research, Research into Ageing, Help the Aged, and the EPSRC Challenging Engineering Program in collaboration with the Institute of Mechanobiological Engineering, Leeds.

**Acknowledgments:** In dedication to F.G.E. Pautard (former joint founding editor of Calcified Tissue Research), who considered that "Today's biology contains all the steps in its origins"; if the above amounts to anything, it's your doing. Also, P.J. Meunier (Lyons) for training in hard tissue technology, and H.K. Kashiwa (Washington), whose application of stain technology to osteogenic cells was inspirational. Mentors: Departmental heads B.E. Christopher Nordin (Leeds), John A. Kanis (Sheffield), David R. Johnson (Leeds), James Moore (Leeds), and Alan Wright (Bradford). Contributing as research team members were the following postdoctoral scientists: D. Howard Carter who never ceased to amaze me (noncollagenous protein immunohistochemistry and antigenicity, bone and dentine substructure, cryomicroscopy and slam freezing, aided by X-ray microanalysis with Paul Hatton, Sheffield); Kathryn M. Linton (prokaryote model, age-related disease); Valerie Fallon (bone and protozoan cell culture, Golgi apparatus transfection and GFP-fluorescence); Aiman I Al-Quaitat, Jordan (hard and soft tissue mineral particles); Philippa E. Garner (protozoan model, osteocyte networks, trabecular termini, computer-assisted analysis); S. Mohsen Shahtaheri, Iran (trabecular microarchitecture in pregnancy and lactation, osteocalcin immunohistochemistry); Freide Luther (immunohistochemistry and ovariectomy.) Also is the significant input of comprehensively funded visiting overseas orthopaedic surgeons, including Hitoshi Saino, from Sapporo Japan (immunohistochemistry and physical activity) and Mizuo Itoda (trabecular microarchitecture, microCT and alendronate), together with clinicians Lucia Stasiak, Warsaw, Kamala Sagreiya, Delhi and Darinka Dekanic, Zagreb (calcification front microscopy) and maxillofacial surgeon Martin Chin, San Fransisco (periostal Sharpey's fibre). Also, the long-term clinical and histological input of Leeds consultant rheumatologist Leslie D. Hordon and the orthopaedic surgeons at Dewsbury District Hospital. Not underestimated is the contribution of Faculty of Biology undergraduates, including Jaqueline Allen (protozoan cell model); David Stoker (fish scale bone); Melanie J.D. Cowdy (Khourigba phosphate microscopy); Charles Tapping (microbiology); Andrew Hartopp (cancellous bone microanalysis). All were supported by laboratory manager Patricia A. Shore, elemental microanalyst Roger C. Shore, microbiologist David G. Adams, biomechanical engineer Ruth Wilcox, veterinarians Anthony Care and Tim Skerry, IT image analyst Steven Paxton, statistician Terry Mc Andrew, chemist Linda Cattley, botanist Naomi Makins. "Keeping wheels turning" were Richard Milner, Len Sanderson, and an essential group of MRC Mineral Metabolism Unit clinicians, including M. Peacock, J.C. Gallagher, and M. Cochran, whose patients donated pathological iliac crest bone biopsies for many years, for comparison with a unique normal autopsy collection from Leeds General Infirmary.

**Conflicts of Interest:** The authors declare no conflict of interest.

## References

1. Aaron, J.E.; Rogers, J.; Kanis, J.A. Paleohistology of Paget's disease in two medieval skeletons. *Am. J. Phys. Anthr.* **1992**, *89*, 325–331. [CrossRef] [PubMed]
2. Aaron, J.E.; Makins, N.B.; Caple, I.W.; Abbas, S.K.; Pickard, D.W.; Care, A.D. The parathyroid glands in the skeletal development of the ovine foetus. *Bone Miner.* **1989**, *7*, 13–22. [CrossRef] [PubMed]
3. Aaron, J.E. Histology and Micro-anatomy of Bone. In *Calcium, Phosphate and Magnesium Metabolism*; Nordin, B.E.C., Ed.; Churchill Livingstone: Edinburgh, Scotland, 1976; pp. 298–356.
4. Kashiwa, H.K. Calcium phosphate in osteogenic cells. *Clin. Orthop.* **1970**, *70*, 200–212. [CrossRef] [PubMed]
5. Lester, K.S.; Ash, M.M. Scanning electron microscopy of mineralised cartilage in rat mandibular condyle. *J. Ultrastruct. Res.* **1980**, *72*, 141–150. [CrossRef]
6. Carter, D.H.; Hatton, P.V.; Aaron, J.E. The ultrastructure of slam frozen bone mineral. *Histochem. J.* **1997**, *9*, 783–793. [CrossRef]
7. Carter, D.H. An Immunohistochemical and Morphological Study of Trabecular Generation: Role of the Extracellular Matrix. Ph.D. Thesis, University of Leeds, Leeds, UK, 1995.
8. Termine, J.D.; Posner, A.S. Amorphous/crystalline interrelationships in bone mineral. *Calcif. Tissue Res.* **1967**, *1*, 8–23. [CrossRef]
9. Davies, J.E.; Chernecky, R.; Lowenberg, B.; Shiga, A. Deposition and resorption of calcified matrix in vitro by rat marrow cells. *Cells Mater.* **1991**, *1*, 3–15.
10. Pautard, F.G.E. Mineralization of keratin and its comparison with the enamel matrix. *Nature* **1963**, *199*, 531–535. [CrossRef]
11. Pautard, F.G.E. Calcium phosphate and the origin of backbones. *New Sci.* **1961**, *12*, 364–366.
12. Aaron, J.E. Periosteal Sharpey's fibres: A novel bone matrix regulatory system? *Front. Endocrinol.* **2012**, *3*, 98. [CrossRef]
13. Queckett, J. On the intimate structure of bone. *Trans. Microsc. Soc. Lond.* **1846**, *2*, 46–58.
14. Pommer, G. *Untersuchungen uber Osteomalacie und Rachitis*; Vogel: Leipzig, Germany, 1885.
15. Hancox, N.M. *Biology of Bone*; Cambridge University Press: Cambridge, UK, 1972.
16. Pautard, F.G.E. Phosphorus and bone. In *New Trends in Bio-Inorganic Chemistry*; Williams, R.J.P., Da Silva, J.R.R.F., Eds.; Academic Press: London, UK; New York, NY, USA; San Francisco, CA, USA, 1978; pp. 261–354.
17. Ingber, D.E. Tensegrity I. Cell structure and hierarchical systems in biology. *J. Cell Sci.* **2003**, *116*, 1157–1173. [CrossRef] [PubMed]

18. Sharpey, W.; Thompson, A.; Cleland, J. *Quain's Elements of Anatomy*, 7th ed.; James Walton: London, UK, 1867.
19. Carter, D.H.; Sloan, P.; Aaron, J.E. Immunolocalization of collagen types 1 and 11, tenascin and fibronectin in intramembranous bone. *J. Histochem. Cytochem.* **1991**, *39*, 599–606. [CrossRef]
20. Aaron, J.E.; Carter, D.H. Rapid preparation of fresh frozen undecalcified bone for histology and histochemical analysis. *J. Histochem. Cytochem.* **1987**, *35*, 361–369. [CrossRef]
21. Aaron, J.E.; de Vernejoul, M.-C.; Kanis, J.A. Bone hypertrophy and trabecular generation in Paget's disease and in fluoride-treated osteoporosis. *Bone Miner.* **1992**, *17*, 399–413. [CrossRef]
22. Luther, F.; Saino, H.; Carter, D.H.; Aaron, J.E. Evidence for an extensive collagen type III/VI proximal domain in the rat femur I. Diminution with ovariectomy. *Bone* **2003**, *32*, 652–659. [CrossRef] [PubMed]
23. Luther, F. Bone Atrophy, Trabecular Architecture and Matrix Proteins. Ph.D. Thesis, University of Leeds, Leeds, UK, 1998.
24. Wronski, T.J.; Morey, E.R. Effect of spaceflight on periosteal bone formation in rats. *Am. J. Physiol.* **1983**, *424*, R305–R309. [CrossRef] [PubMed]
25. Saino, H.; Luther, F.; Carter, D.H.; Natali, A.J.; Turner, D.L.; Shahtaheri, M.; Aaron, J.E. Evidence for an extensive collagen type III proximal domain in the rat femur II. Expansion with exercise. *Bone* **2003**, *32*, 660–668. [CrossRef] [PubMed]
26. Aaron, J.E.; Skerry, T.M. Intramembranous trabecular generation in normal bone. *Bone Miner.* **1994**, *25*, 211–230. [CrossRef]
27. Aaron, J.E. Bone turnover and microdamage. *Adv. Osteoporotic Fract. Manag.* **2003**, *2*, 102–110.
28. Aaron, J.E.; Johnson, D.R.; Kanis, J.A.; Oakley, B.A.; O'Higgins, P.; Paxton, S.K. An automated method for the analysis of trabecular bone structure. *Comput. Biomed. Res.* **1992**, *25*, 1–16. [CrossRef] [PubMed]
29. Aaron, J.E.; Shore, P.A. Bone histomorphometry. Concepts and common techniques. In *Handbook of Histology Methods for Bone and Cartilage*; An, Y.H., Martin, K.L., Eds.; Humana Press: Totowa, NJ, USA, 2003; pp. 331–351.
30. Shore, P.A.; Shore, R.C.; Aaron, J.E. A three-dimensional histological method for direct determination of the number of trabecular termini in cancellous bone. *Biotech. Histochem.* **2000**, *75*, 183–192. [CrossRef] [PubMed]
31. Aaron, J.E.; Shore, P.A.; Shore, R.C.; Kanis, J.A. Trabecular architecture in women and men of similar bone mass with and without vertebral fracture: II. Three dimensional histology. *Bone* **2000**, *27*, 277–282. [CrossRef] [PubMed]
32. Hordon, L.D.; Raisi, M.; Aaron, J.E.; Paxton, S.K.; Beneton, M.; Kanis, J.A. Trabecular architecture in women and men of similar bone mass with and without fracture: I. Two dimensional histology. *Bone* **2000**, *27*, 271–276. [CrossRef] [PubMed]
33. Garner, P.; Wilcox, R.; Hordon, L.D.; Aaron, J.E. A direct computer-assisted method for the spatial 3D mapping of trabecular termini in the spine. *IBMS BoneKEy* **2013**, *10*, SS14.
34. Aaron, J.E.; Shore, P.A.; Itoda, M.; Morrison, R.J.M.; Hartopp, A.; Hensor, E.M.A.; Hordon, L.D. Mapping trabecular disconnection "hotspots" in aged human spine and hip. *Bone* **2015**, *78*, 71–80. [CrossRef] [PubMed]
35. Hordon, L.D.; Itoda, M.; Shore, P.A.; Shore, R.C.; Heald, M.; Brown, M.; Kanis, J.A.; Rodan, G.A.; Aaron, J.E. Preservation of thoracic spine microarchitecture by alendronate: Comparison of histology and microCT. *Bone* **2006**, *38*, 444–449. [CrossRef] [PubMed]
36. Hodgkinson, A.; Aaron, J.E.; Horsman, A.; McLachlan, M.S.F.; Nordin, B.E.C. Effect of oophorectomy and calcium deprivation on bone mass in the rat. *Clin. Sci. Mol. Med.* **1978**, *54*, 439–446. [CrossRef] [PubMed]
37. Pautard, F.G.E. Calcium phosphate microspheres in biology. *Prog. Cryst. Growth Charact.* **1981**, *4*, 89–98. [CrossRef]
38. Eanes, E.D.; Termine, J.D.; Nylen, M.U. An electron microscopic study of the formation of calcium phosphate and its transformation to crystalline apatite. *Calcif. Tissue Res.* **1973**, *12*, 143–158. [CrossRef]
39. Termine, J.D.; Eanes, E.D. Calcium phosphate deposition from balanced salt solutions. *Calcif. Tissue Res.* **1974**, *15*, 81–84. [CrossRef]
40. Greenfield, D.J.; Eanes, E.D. Formation chemistry of amorphous calcium phosphate prepared from carbonate containing solutions. *Calcif. Tissue Res.* **1972**, *9*, 152–162. [CrossRef] [PubMed]
41. Aaron, J.E. Histological Aspects of Vitamin D and Bone. In *Vitamin D*; Lawson, D.E.M., Ed.; Academic Press: London, UK, 1978; pp. 201–265.
42. Bien, S.M. High hydrostatic pressure effects on *Spirostomum ambiguum*. *Calcif. Tissue Res.* **1967**, *1*, 170–172. [CrossRef] [PubMed]
43. Pautard, F.G.E. Calcification in Unicellular Organisms. In *Biological Calcification, Cellular and Molecular Aspects*; Schraer, H., Ed.; Appleton-Century-Crofts: New York, NY, USA, 1970; pp. 105–201.
44. Fallon, V.; Garner, P.E.; Aaron, J.E. Mineral fabrication and golgi apparatus activity in *Spirostomum ambiguum*: A primordial paradigm of the stressed bone cell? *J. Biomed. Sci. Eng.* **2017**, *10*, 466–483. [CrossRef]
45. Aaron, J.E. Osteocyte types in the developing mouse calvarium. *Calcif. Tissue Res.* **1973**, *12*, 259–279. [CrossRef]
46. Fallon, V.; Carter, D.H.; Aaron, J.E. Mineral fabrication and golgi apparatus activity in the mouse calvarium. *J. Biomed. Sci. Eng.* **2014**, *7*, 769–779. [CrossRef]
47. Fallon, V. The Fabrication of Mineral Particles by Bone Cells and Unicellular Organisms. Ph.D. Thesis, University of Leeds, Leeds, UK, 2006.
48. Matthews, J.L.; Martin, J.H.; Sampson, H.W.; Kunin, A.S.; Roan, J.H. Mitochondrial granules in the normal and rachitic rat epiphysis. *Calcif. Tissue Res.* **1970**, *5*, 91–99. [CrossRef]
49. Aaron, J.E. Cellular ubiquity of calcified microspheres: A matter of degree, ancient history and the golgi body. *J. Biomed. Sci.* **2016**, *5*, 3–7. [CrossRef]

50. Wilbur, K.M.; Watabe, N. Experimental studies on calcification in molluscs and the alga *Coccolithus huxleyi*. *Ann. N. Y. Acad. Sci.* **1963**, *109*, 82–112. [CrossRef]
51. Manton, I.; Leedale, G.F. Observations on the micro-anatomy of *Crystallolithus hyalinus* Gaardner and Markali. *Arch. Microbiol.* **1963**, *47*, 115–136.
52. Outka, D.E.; Williams, D.C. Sequential coccolith morphogenesis in *Hymenomonas carterae*. *J. Protozool.* **1971**, *18*, 285–297. [CrossRef]
53. Aaron, J.E. The Development of the Bone Cell and its Role in Mineralisation and Resorption. Ph.D. Thesis, University of Leeds, Leeds, UK, 1974.
54. Aaron, J.E.; Pautard, F.G.E. Ultrastructural features of phosphate in developing bone cells. *Isr. J. Med. Sci.* **1972**, *8*, 625–629.
55. Aaron, J.E.; Pautard, F.G.E. A cell cycle in bone mineralization. In *The Cell Cycle in Development and Differentiation*; Balls, M., Billett, F.S., Eds.; Cambridge University Press: Cambridge, UK, 1973; pp. 325–330.
56. Aaron, J.E.; Pautard, F.G.E. Studies of bone in vivo by incident light interference contrast microscopy. In *Proceedings of the IXth European Symposium on Calcified Tissues, Vienna, Austria, October 1972*; Czitober, H., Eschberger, J., Eds.; Facta Publications: Vienna, Austria, 1973; pp. 197–201.
57. Aaron, J.E.; Pautard, F.G.E. Tetracycline staining of bone in normal and pathological states. In *Calcium Metabolism, Bone and Metabolic Bone Diseases*; Kuhlencordt, F., Kruse, H.P., Eds.; Springer-Verlag: Berlin, Germany, 1975; pp. 211–217.
58. Aaron, J.E. Demineralization of bone in vivo and in vitro: Evidence for a microskeletal arrangement. *Metab. Bone Dis. Relat. Res.* **1980**, *25*, 109–116.
59. Aaron, J.E. Alkaline phosphatase, vesicles and calcification. *Metab. Bone Dis. Relat. Res.* **l980**, *2*, l51–157.
60. Park, H.Z.; Kashiwa, H.K. Calcium localized in juxtanuclear granules of epiphyseal chondrocytes with a dilute glyoxal bis(2-hydroxyanil) solution. *Calcif. Tissue Res.* **1975**, *19*, 189–197. [CrossRef]
61. Kashiwa, H.K.; Thiersch, N.J. Evaluation of potassium pyroantimonate for localizing calcium bound to organic compounds in epiphyseal chondrocytes. *J. Histochem. Cytochem.* **1984**, *32*, 1055–1065. [CrossRef]
62. Jayasinghe, J.A.P.; Jones, S.J.; Boyde, A. Scanning electron microscopy of human lumbar vertebral trabecular bone surfaces. *Virchows Arch. A* **1993**, *422*, 25–34. [CrossRef] [PubMed]
63. Rungby, J.; Kassem, M.; Eriksen, E.F.; Danscher, G. The von Kossa reaction for calcium deposits: Silver lactate staining increases sensitivity and reduces background. *Histochem. J.* **1993**, *25*, 446–451. [CrossRef]
64. Kawamata, S. The distribution of calcium in undecalcified bone as revealed by an improved pyroantimonate method. *Histochem. J.* **1992**, *24*, 275–282. [CrossRef]
65. Wooding, F.B.P.; Morgan, G. Calcium localization in lactating rabbit mammary secretory cells. *J. Ultrastruct. Res.* **1978**, *63*, 323–333. [CrossRef]
66. Garner, P.; Wilcox, R.; Hordon, L.D.; Aaron, J.E. Quantification of cell networks: Computer-assisted method for 3D mapping of osteocyte populations in the ageing human femur. *IBMS BoneKEy* **2013**, *10*, S26. [CrossRef]
67. Garner, P.E.; Wilcox, R.; Hordon, L.D.; Aaron, J.E. Mapping biomechanical diversity in the osteocyte syncytium: A novel automated 3D method applied to the femur. *Bone* **2025**. *in preparation*.
68. Garner, P.E. Bone Ageing and Strutural Disconnection. Ph.D. Thesis, University Leeds, Leeds, UK, 2009.
69. Carter, D.H.; Sloan, P.; Aaron, J.E. Trabecular generation de novo: An immunohistochemical study of the human femoral anlagen. *Anat. Embryol.* **1992**, *186*, 229–240. [CrossRef] [PubMed]
70. Aaron, J.E.; Oliver, B.; Clark, N.; Carter, D.H. Calcified microspheres as biological entities and their isolation from bone. *Histochem. J.* **1999**, *31*, 455–470. [CrossRef]
71. Ingber, D.E.; Folkman, J. Mechanochemical switching between growth and differentiation during fibroblast growth factor-stimulated angiogenesis. *J. Cell Biol.* **1989**, *109*, 317–330. [CrossRef]
72. Bianco, P.; Riminucci, M.; Silvestrini, G.; Bonucci, E.; Termine, J.D.; Fisher, L.K.; Gehron-Robey, P. Localisation of bone sialoprotein (BSP) to golgi and post-golgi secretory structures in osteoblasts and to discrete sites in early bone matrix. *J. Histochem. Cytochem.* **1993**, *41*, 193–203. [CrossRef] [PubMed]
73. Appleton, J. Ultrastructural observations on the inorganic/organic relationships in early cartilage calcification. *Calcif. Tissue Res.* **1971**, *7*, 307–317. [CrossRef] [PubMed]
74. Carter, D.H.; Scully, A.J.; Davies, R.M.; Aaron, J.E. Evidence for phosphoprotein microspheres in bone. *Histochem. J.* **1998**, *30*, 677–686. [CrossRef] [PubMed]
75. Shahtaheri, S.M.; Aaron, J.E.; Oakley, B.A. Immunolocalization of osteocalcin in calcified microspheres in lamb vertebrae and mouse bones using PAP method. In Proceedings of the ECTS and ASBM Joint Symposium, 2002. Available online: https://ectsoc.org/pastcongress/zagreb2002/poster1.htm (accessed on 19 August 2024)
76. Shahtaheri, S.M. Microanatomy of Trabecular Bone during Pregnancy. Ph.D. Thesis, University of Leeds, Leeds, UK, 1997.
77. Aaron, J.E. Autoclasis—A mechanism of bone resorption and an alternative explanation for osteoporosis. *Calcif. Tissue Res.* **1977**, *22*, 247–254. [CrossRef]
78. Yamamoto, T.; Nagai, H. Tartrate-resistant acid phosphatase accumulated in the matrix of developing medullary bone. *J. Bone Miner. Res.* **1994**, *9*, 1153–1157. [CrossRef]
79. Aaron, J.E. Cellular ubiquity of calcified microspheres: A matter of degree, ancient history and the golgi body. In *Top 10 Contributions on Biomedical Sciences*, 2nd ed.; AvidScience: Hyderabad, India, 2018; pp. 2–14. [CrossRef]

80. Aaron, J.E.; Shore, P.A. Histomorphometry. In *The Physical Measurement of Bone*; Langton, C.M., Njeh, C.F., Eds.; Institute of Physics Publishing: Bristol, UK; Philadelphia, PA, USA, 2004; pp. 185–224.
81. Aaron, J.E.; Shore, P.A. Microscopy and related techniques. In *The Physical Measurement of Bone*; Langton, C.M., Njeh, C.F., Eds.; Institute of Physics Publishing: Bristol, UK; Philadelphia, PA, USA, 2004; pp. 225–264.
82. Ali, S.Y.; Sajdera, S.W.; Anderson, H.C. Isolation and characterisation of calcifying matrix vesicles from epiphyseal cartilage. *Proc. Nat. Acad. Sci. USA* **1970**, *67*, 1513–1520. [CrossRef]
83. De Bernard, B.; Furlan, G.; Stagni, N.; Vittur, F.; Zanetti, M. Role of a calcium binding glycoprotein in the calcification process. *Calcif. Tissue Res.* **1977**, *22*, 191–196. [CrossRef]
84. Nylen, M.U.; Eanes, E.D.; Termine, I.D. Molecular and ultrastructural studies of non-crystalline calcium phosphates. *Calcif. Tissue Res.* **1972**, *9*, 95–108. [CrossRef] [PubMed]
85. Ennever, J.; Creamer, H. Microbiologic calcification: Bone mineral and bacteria. *Calcif. Tissue Res.* **1967**, *1*, 87–93. [CrossRef] [PubMed]
86. Carlisle, E.M. A requirement in bone formation independent of vitamin D. *Calcif. Tissue Int.* **1981**, *33*, 27–34. [CrossRef] [PubMed]
87. Linton, K.M.; Tapping, C.R.; Adams, D.G.; Carter, D.H.; Shore, R.C.; Aaron, J.E. A silicon cell cycle in a bacterial model of calcium phosphate mineralogenesis. *Micron* **2013**, *44*, 419–432. [CrossRef] [PubMed]
88. Linton, K.M. Calcium Phosphate Morphology in Bone and Bacterium. Ph.D. Thesis, University of Leeds, Leeds, UK, 2007.
89. Landis, W.J.; Glimcher, M.J. Electron optical and analytical observations of rat growth plate cartilage prepared by ultracryomicrotomy. *J. Ultrastruct. Res.* **1982**, *78*, 227–268. [CrossRef]
90. Atkin, I.; Omoy, A. Transplacental effects of cortisone acetate on calcification and ossification of long bones in mice. *Metab. Bone Dis. Relat. Res.* **1981**, *3*, 199–207. [CrossRef]
91. Arnott, H.J.; Pautard, F.G.E. The inorganic phase of bone: A reappraisal. *Calcif. Tissue Res.* **1968**, *2*, 2. [CrossRef]
92. Arnott, H.J.; Pautard, F.G.E. Calcification in unicellular organisms. Also, Calcification in plants. In *Biological Calcification. Cellular and Molecular Aspects*; Schraer, H., Ed.; Appleton-Century-Crofts: New York, NY, USA, 1970; pp. 105–201 and 375–446.
93. Carter, D.H.; Scully, A.J.; Heaton, D.A.; Young, M.P.; Aaron, J.E. Effect of deproteination on bone mineral morphology: Implications for biomaterials and aging. *Bone* **2002**, *31*, 389–395. [CrossRef]
94. Skerry, T.M.; Bitensky, L.; Chayen, J.; Lanyon, L.E. Early strain-related changes in enzyme activity in osteocytes following bone loading in vivo. *J. Bone Miner. Res.* **1989**, *4*, 783–786. [CrossRef]
95. Al-Quaitat, A. Anatomy of Sharpey's Fibres and Their Calcification with Age. Master's Thesis, University of Leeds, Leeds, UK, 2004.
96. Al-Qtaitat, A.; Shore, R.C.; Aaron, J.E. Structural changes in the ageing periosteum using collagen III immunostaining and chromium labelling as indicators. *J. Musculoskelet. Neuronal Interact.* **2010**, *10*, 112–123.
97. Al-Qtaitat, A. The Mineral Phase: Calcified Microsphere Populations in Young and Ageing Hard and Soft Tissues. Ph.D. Thesis, University of Leeds, Leeds, UK, 2007.
98. Chin, M.; Aaron, J.E. Sharpey biologic model for bone formation. In *The Sinus Bone Graft*, 3rd ed.; Jensen, O.T., Ed.; Quintessence Publishing: London, UK; Paris, France; Berlin, Germany, 2019; pp. 213–226.
99. Aaron, J.E.; Francis, R.M.; Peacock, M.; Makins, N.B. Contrasting microanatomy of idiopathic and corticosteroid-induced osteoporosis. *Clin. Orthop.* **1989**, *243*, 294–305. [CrossRef]
100. Shahtaheri, S.M.; Aaron, J.E.; Johnson, D.R.; Paxton, S.K. The impact of mammalian reproduction on cancellous bone architecture. *J. Anat.* **1999**, *194*, 407–421. [CrossRef] [PubMed]
101. Shahtaheri, S.M.; Aaron, J.E.; Johnson, D.R.; Purdie, D.W. Changes in trabecular bone architecture in women during pregnancy. *BJOG Int. J. Obstet. Gynaecol.* **1999**, *106*, 432–438. [CrossRef]
102. Shore, P.A.; Shore, R.C.; Aaron, J.E. Floating bone segments: A legacy of trabecular disconnection "hotspots", cross strut microdamage and cancellous "crumple zones". *J. Biomed. Sci. Eng.* **2023**, *16*, 65–79. [CrossRef]
103. Linton, K.M.; Hordon, L.D.; Shore, R.C.; Aaron, J.E. Bone mineral "quality": Differing characteristics of calcified microsphere populations at the osteoporotic and osteoarthritic femoral articulation front. *J. Biomed. Sci. Eng.* **2014**, *7*, 739–755. [CrossRef]
104. Meunier, P.; Aaron, J.E.; Edouard, C.; Vignon, G. Osteoporosis and the replacement of cell populations of the marrow by adipose tissue. *Clin. Orthop.* **1971**, *80*, 147–154. [CrossRef]
105. Aaron, J.E.; Gallagher, J.C.; Nordin, B.E.C. Seasonal variation of histological osteomalacia in femoral-neck fractures. *Lancet* **1974**, *2*, 84–85. [CrossRef]
106. Burton, F.G.; Neuman, M.W.; Neuman, W.F. On the possible role of crystals in the origins of life. I. The adsorption of nucleosides, nucleotides and pyrophosphate by apatite crystals. *Biosystems* **1969**, *3*, 20–26. [CrossRef]
107. Burton, F.G.; Neuman, M.W.; Neuman, W.F. On the possible role of crystals in the origins of life. II. The adsorption of amino acids by apatite crystals. *Biosystems* **1969**, *3*, 69–73. [CrossRef]
108. Pautard, F.G.E. The molecular-biologic background to the evolution of bone. *Clin. Orthop.* **1962**, *24*, 230–244.
109. Pautard, F.G.E. The structure and genesis of calcium phosphates in vertebrates and invertebrates. In *Physico-Chemie et Crystallographie des Apatites d'Interet Biologique*; Colloques Internationaux CNRS: Paris, France, 1975; Volume 230, pp. 93–100.
110. Pautard, F.G.E. Hydroxyapatite as a developmental feature of *Spirostomum ambiguum*. *Biochim. Biophys. Acta* **1959**, *35*, 33–46. [CrossRef]

111. Wong, M.; Carter, D.R. A theoretical model of endochondral ossification and bone architectural construction in long bone ontogeny. *Anat. Embryol.* **1990**, *181*, 523–532. [CrossRef]
112. Compston, J.E. Connectivity of cancellous bone: Assessment and mechanical implications. *Bone* **1994**, *15*, 463–466. [CrossRef]
113. Tabor, Z.; Rokila, E. Comparison of trabecular architecture in young and old bones. *Med. Phys.* **2000**, *27*, 1165–1173. [CrossRef] [PubMed]
114. Thomsen, J.S.; Ebbesen, E.N.; Mosekilde, L. Age-related differences between thinning of horizontal and vertical trabeculae in human lumbar bone as assessed by a new computerized method. *Bone* **2002**, *31*, 136–142. [CrossRef] [PubMed]
115. Keaveney, T.M.; Yeh, O.C. Architecture and trabecular bone—Towards an improved understanding of the biomechanical effects of age, sex and osteoporosis. *J. Musculoskelet. Neuronal. Interact.* **2002**, *3*, 205–208.
116. Sverdlova, N. Tensile trabeculae—Myth or reality? *J. Musculoskelet. Neuronal Interact.* **2011**, *11*, 1–7.
117. Odgaard, A.; Gunderson, H.J.G. Quantification of connectivity in cancellous bone with special emphasis on 3-D reconstruction. *Bone* **1993**, *14*, 173–182. [CrossRef]
118. Raggio, C.L.; Boyan, B.D.; Boskey, A.L. In vivo hydroxyapatite formation induced by lipids. *J. Bone Miner. Res.* **1986**, *1*, 409–416. [CrossRef]
119. Glimcher, M.J. Mechanisms of calcification in bone: Role of collagen fibrils and collagen-phosphoprotein complexes in vitro and in vivo. *Anat. Rec.* **1989**, *224*, 139–153. [CrossRef]
120. Chang, Y.L.; Stanford, C.M.; Keller, J.C. Calcium and phosphate supplementation promotes bone cell mineralization: Implications for hydroxyapatite (HA)-enhanced bone formation. *J. Biomed. Mater. Res.* **2000**, *52*, 270–280. [CrossRef]
121. Damen, J.J.M.; Ten Cate, J.M. Silica-induced precipitation of calcium phosphate in the presence of inhibitors of hydroxyapatite formation. *J. Dent. Res.* **1992**, *71*, 453–457. [CrossRef]
122. Cazalbou, S.; Combes, C.; Eichert, D.; Rey, C.; Glimcher, M.J. Poorly crystalline apatites: Evolution and maturation in vitro and in vivo. *J. Bone Miner. Metab.* **2004**, *22*, 310–317. [CrossRef] [PubMed]
123. Bachra, B.N. Calcification in vitro of collagenous model systems. Chemical and electron microscopic aspects. *Calcif. Tissue Res.* **1970**, *4*, 31–34. [CrossRef]
124. Arsenault, A.L.; Frankland, B.W.; Ottensmeyer, F.P. Vectorial sequence of mineralisation in the turkey leg tendon determined by electron microscopy imaging. *Calcif. Tissue Int.* **1991**, *48*, 46–55. [CrossRef]
125. Marino, A.A.; Becker, R.O. Evidence for epitaxy in the formation of collagen and apatite. *Nature* **1970**, *226*, 652–653. [CrossRef]
126. Eanes, E.D.; Termine, J.; Posner, A. Amorphous calcium phosphate in skeletal tissues. *Clin. Orthop. Relat. Res.* **1967**, *53*, 223–235. [CrossRef]
127. Glimcher, M.J.; Bonar, L.C.; Grynpas, M.D.; Landis, W.J.; Roufosse, A.H. Recent studies of bone mineral: Is the amorphous calcium phosphate theory valid? *J. Cryst. Growth* **1981**, *53*, 100–119. [CrossRef]
128. Anderson, H.C. Molecular biology of matrix vesicles. *Clin. Orthop. Relat. Res.* **1995**, *314*, 266–280. [CrossRef]
129. Barragan-Adjemian, C.; Nicolella, D.; Dusevich, V.; Dallas, M.R.; Eick, J.D.; Bonewald, L.F. Mechanisms by which MLO-A5 late osteoblasts/early osteocytes mineralize in culture; similarities with mineralisation of lamellar bone. *Calcif. Tissue Int.* **2006**, *79*, 340–353. [CrossRef] [PubMed]
130. Felix, R.; Fleisch, H. The role of matrix vesicles in calcification. *Fed. Proc.* **1976**, *35*, 169–171. [PubMed]
131. Anderson, H.C.; Sipe, J.B.; Hessle, L.; Dhanyamraju, R.; Atti, E.; Camacho, N.P.; Milan, J.L. Impaired calcification around matrix vesicles of growth plate and bone in alkaline-phosphate-deficient mice. *Am. J. Pathol.* **2004**, *164*, 841–847. [CrossRef] [PubMed]
132. Hirschmann, P.N.; Nichols, G. The isolation and partial characterisation of a calcium-rich particulate fraction from bone cells. *Calcif. Tissue Res.* **1972**, *9*, 67–79. [CrossRef] [PubMed]
133. Mikuni-Takagaki, Y.; Kakai, Y.; Satoyoshi, M.; Kawano, E.; Suzuki, Y.; Kawasi, T.; Sato, S. Matrix mineralization and the differentiation of osteocyte-like cells in culture. *J. Bone Miner. Res.* **1995**, *10*, 231–242. [CrossRef] [PubMed]
134. Bonucci, E.; Silvestrini, G.; Di Grezia, R. The ultrastructure of the inorganic phase associated with the inorganic substance in calcified tissues. *Clin. Orthop. Relat. Res.* **1988**, *233*, 243–261. [CrossRef]
135. Shahtaheri, M.S. Immunolocalization of osteocalcin in calcified microspheres in adult mouse bone using FITC labelling. *Bone* **2001**, *28*, S108.
136. Bonewald, L.F. Osteocytes as dynamic multifunctional cells. *Ann. N. Y. Acad. Sci.* **2007**, *1116*, 28–90. [CrossRef] [PubMed]
137. Bonucci, E. Crystal ghosts and biological mineralization: Fancy spectres in an old castle or neglected structures worthy of belief? *J. Bone Miner. Metab.* **2002**, *20*, 249–265. [CrossRef]
138. Osborn, D.; Hamilton, T.C. Electron microbeam analysis of calcium distribution in the ciliated protozoan *Spirostomum ambiguum*. *J. Cell. Physiol.* **1976**, *91*, 409–416. [CrossRef]
139. Sanchez-Navas, A.; Martin-Algarra, A. Genesis of apatite in phosphate stromatolites. *Eur. J. Miner.* **2001**, *13*, 361–367. [CrossRef]
140. Martin, J.H.; Mathews, J.L. Mitochondrial granules in chondrocytes, osteoblasts and osteocytes. *Clin. Orthop.* **1970**, *68*, 273–278. [CrossRef] [PubMed]
141. Halstead, L.B. Are mitochondria directly involved in bone mineralization? The mitochondria and the origin of bone. *Calcif. Tissue Res.* **1969**, *3*, 103–104. [CrossRef]
142. Ooi, S.W.; Smillie, A.C.; Kardos, T.B.; Shepherd, M.G. Intracellular mineralisation of *Bacterionema matruchotti*. *Can. J. Microbiol.* **1981**, *27*, 267–270. [CrossRef] [PubMed]

143. Ho, A.M.; Johnson, M.D.; Kingsley, D.M. Role of the mouse *ank* gene in control of tissue calcification and arthritis. *Science* **2000**, *289*, 265–270. [CrossRef] [PubMed]
144. Allan, V.J.; Kreis, T.E. A microtubule-binding protein associated with the Golgi apparatus. *J. Cell Biol.* **1986**, *102*, 2229–2239. [CrossRef] [PubMed]
145. Farquhar, M.; Palude, G.E. The Golgi apparatus: 100 years of progress and controversy. *Trends Cell Biol.* **1998**, *8*, 2–10. [CrossRef]
146. Mollenhauer, H.H.; Morre, D.J. Perspectives on Golgi apparatus form and function. *J. Electron Microsc. Tech.* **1991**, *17*, 2–14. [CrossRef]
147. Cameron, D.A. The Golgi apparatus in bone and cartilage cells. *Clin. Orthop.* **1968**, *58*, 191–211. [CrossRef]

**Disclaimer/Publisher's Note:** The statements, opinions and data contained in all publications are solely those of the individual author(s) and contributor(s) and not of MDPI and/or the editor(s). MDPI and/or the editor(s) disclaim responsibility for any injury to people or property resulting from any ideas, methods, instructions or products referred to in the content.